

Structures and stability of the Cu₃₈ cluster at finite temperature

César Castillo-Quevedo,¹ Edgar Paredes-Sotelo,² Carlos Emiliano Buelna-García,² Edwin Rene Hoil-Canul,³ Jhonny Robert Mis-May,³ Jarbin Barrios-Díaz,³ Martha Fabiola Martín-del-Campo-Solis,¹ Edgar Zamora-Gonzalez,¹ Adolfo López-Sánchez,³ Jesús Ramón Cob-Cantu,³ Jorge Briceño-Mena,³ Freddy Francisco Agustín-Argüello,³ Tzarara López-Luke,⁴ Gerardo Martínez-Guajardo,^{5,*} and Jose Luis Cabellos^{6,†}

¹Departamento de Fundamentos del Conocimiento,
Centro Universitario del Norte, Universidad de Guadalajara,
Carretera Federal No. 23, Km. 191, C.P. 46200, Colotlán, Jalisco, México

²Departamento de Investigación en Polímeros y Materiales,
Edificio 3G. Universidad de Sonora. Hermosillo, Sonora, México

³Universidad Politécnica de Tapachula, Carretera Tapachula a Puerto Madero km 24+300,
San Benito, Puerto Madero C.P. 30830, Tapachula, Chiapas, México

⁴Instituto de Investigación en Metalurgia y Materiales,
Universidad Michoacana de San Nicolás de Hidalgo, Edificio U,
Ciudad Universitaria, Morelia, Mich., 58030, México

⁵Unidad Académica de Ciencias Químicas, Área de Ciencias de la Salud,
Universidad Autónoma de Zacatecas, Km. 6 carretera Zacatecas-Guadalajara s/n,
Ejido La Escondida C. P. 98160, Zacatecas, Zac.

⁶Universidad Politécnica de Tapachula, Carretera Tapachula a Puerto Madero km 23+300,
San Benito, Puerto Madero C.P. 30830, Tapachula, Chiapas, México

(Dated: March 22, 2022)

The UV-visible and IR properties of the Cu₃₈ nanocluster depend to a great extent on the temperature. Density functional theory and nanothermodynamics can be combined to compute the geometrical optimization of isomers and their spectroscopic properties in an approximate manner. In this article, we investigate entropy-driven isomer distributions of Cu₃₈ clusters and the effect of temperature on their UV-visible and IR spectra. An extensive, systematic global search is performed on the potential and free energy surfaces of Cu₃₈ using a two-stage strategy to identify the lowest-energy structure and its low-energy neighbors. The effects of temperature on the UV and IR spectra are considered via Boltzmann probability. The computed UV-visible and IR spectrum of each isomer is multiplied by its corresponding Boltzmann weight at finite temperature. Then, they are summed together to produce a final temperature-dependent, Boltzmann-weighted UV-visible and IR spectrum. Additionally, Molecular Dynamics simulation of the Cu₃₈ nanocluster was performed to gain insight into the system dynamics and make a three-dimensional movie of the system with atomistic resolution. Our results show the thermal populations at the absolute temperature of Cu₃₈ cluster, and the disordered structure that dominates at high temperatures.

PACS numbers: 61.46.-w, 65.40.gd, 65., 65.80.-g, 67.25.bd, 71.15.-m, 71.15.Mb, 74.20.Pq, 74.25.Bt, 74.25.Gz, 74.25.Kc

Keywords: Copper clusters, Cu₃₈, density functional theory, temperature, Boltzmann probabilities, Gibbs free energy, entropy, enthalpy, nanothermodynamics, thermochemistry, statistical thermodynamics, genetic algorithm, DFT, Global minimum

I. INTRODUCTION

Nano clusters are of interest due they allow us to study the transition from free atoms to bulk condensed systems¹ as a consequence, analyze the size-dependent evolution of their properties.² Especially, Noble-Metal Nanoclusters (NMC) have attracted attention in many fields of science due to interesting plasmonic, catalytic properties,^{3,4} and photophysical properties at nanoscale.⁵ Particularly, Nano Cu clusters embedded in the dielectric matrix have attracted attention because of their tunable longitudinal surface plasmon resonance.³ Besides, copper is cheaper than gold and silver, and it has large photosensitivity, high thermal and electric conductivity, and optical properties⁶ that makes it a good candidate to develop nanodevices⁷ and nanoelectronics.⁸ In particular, Cu₃₈ attracted at-

tention due to it has a magic structures,⁹ defined in terms of geometric and energetic factors and related to the closing of electronic shells¹⁰ as it happens in small sodium clusters.¹¹ For the Cu₃₈ cluster its magicity is due to only energetic considerations.^{10,12} In contrast, small packed barium clusters with magic numbers, the stability is dominated for geometrical effects rather than electronic effects.¹¹ It is believed that magic structures are the putative global minimum energy structures on the potential energy surface, thus reflect the molecular properties of the system.¹⁰ From the experimental point of view, the Cu₃₈ cluster has been widely studied by photo-electron spectroscopy technique (PES). Pettiette et al.¹³ employing PES extract the electronic gap of anionic Cu₃₈ cluster and found a semiconductor type with 0.33 eV.^{6,13} However, the geometrical structure was not investigated. In contrast, Kostko et al. also studied the anionic Cu₃₈ and from the PES inferred that putative global minimum

should be an oblate structure instead of a high symmetric structure,^{6,14} despite that computations for 38 atom clusters on noble metal clusters frequently found high symmetric (cuboctahedral) structures.^{12,14,15} From the theoretical point of view, Taylor et al. presented a study based on density functional theory (DFT) of thermodynamic properties of Cu₃₈ cluster,¹⁶ Prevoius works employing DFT studied the transition states and reaction energies of water gas shift reaction in a Cu₃₈ cluster and Cu slab.¹⁷ In other previously DFT studies the high symmetry octahedral structure was reported as the lowest energy structure¹⁸ employing PW91¹⁹ functional, plane wave basis set and pseudopotential approximation.²⁰ Hijazi et al.²¹ investigated the Cu₃₈ cluster employing hybrid strategy; they used the embedded atom method potential followed by DFT computations using the PBE functional and pseudopotential approximation and reported that octahedral (OH) symmetry is the putative global minimum structure followed by the incomplete-Mackay icosahedron (IMI) located at 0.26 eV above of the putative global minimum. On the other hand, search for the lowest energy structure employing many body potentials gives a cuboctahedral structure.^{12,22} Erkoc et al.²³ employing an empirical potential-energy function, which contains two-body atomic interactions²⁴ found that the fivefold symmetry appears as putative global minimum in Cu₃₈ cluster. In contrast, the cuboctahedron structure was reported as putative global minimum in a previous studies²⁵ employing empirical *many-body* Gupta and Sutton-Chen potentials. Nevertheless, there has been some discussion which is the lowest energy structure, some previous works consider the Cu₃₈ octahedron cluster, as the putative global minimum^{18,20,21}, in contrast, several others found that Cu₃₈ cluster with the truncated octahedron geometry is energetically more stable than other configurations^{20,21,26–30}. We point out that the energy computed with different methods such as DFT, MP2, or CCSDT, just to mention few of them, yield different energetic ordering.^{31–33} In the case of DFT, the functional and basis set employed, ZPE energy correction, or energy of dispersion among others can interchange the putative global minimum.

Moreover, practical molecular systems and materials needs warm temperature³⁴, so the molecular properties at temperatures T are dominated by Boltzmann distributions of isomers,^{31,35,36} therefore, their properties are statistical averages over the ensemble of conformations.³¹ The structure corresponding to the global minimum ceases to be the most likely at high T so other structures prevail. Furthermore, in small Ag clusters, the temperature leads the transition from the initial FCC phase to other structural modifications,³⁷ so it promotes the changes of fases in materials. Interesting, at different temperatures than zero, the molecular system minimizes the Gibbs free energy and maximizes the entropy.^{31,36}

Although the search of the global and local minima is useful in understanding reactivities and catalytic efficiencies, but such studies most of the

time neglect temperature dependent entropic contributions to free energy when increasing temperature. Taking temperature into account requires dealing with nanothermodynamics.^{31,36,38–43} The thermodynamics of clusters have been studied by a variety of tools,^{31,39,40,44,45} like molecular-dynamics simulations on boron clusters⁴⁶ and Cu₃₈ clusters.⁶ The cluster properties depends strongly of the structure, size, composition, and temperature, so the first step in order to understanding molecular properties is the elucidation of the lowest energy structure and its isomers close in energy.^{28,31,36,41,47,48} This is a complicated task due to several factors.^{31,36} As second step for understanding cluster properties relies on their spectroscopy which gives insight into its structure and it was proposed as a way of detecting structural transformations into clusters. The influence of temperature on the spectroscopy has been computed before for a variety of clusters, for instance,^{31,36,49} such in the present study, for the neutral Cu₃₈ cluster, we use the statistical formulation of thermodynamics or nanothermodynamics^{31,36,39,40} to compute thermodynamics properties and define the putative global minimum at temperatures different from zero, evaluated the relative populations among the isomers and computed UV-Visible and IR spectra as a Boltzmann weighted spectrum sum of individual spectra. Our findings show that at hot temperatures at amorphous structure strongly dominate the putative global minimum whereas the truncated octahedron dominates at cold temperatures. The remainder of the manuscript is organized as follows: Section 2 gives the computational details and a brief overview of the theory and the algorithms used. The results and discussion are presented in section 3; The putative global at room temperature and relative population in ranging temperatures from 20 to 1500K, and the IR spectra as a function of temperature. Conclusions are given in Section 4.

II. THEORETICAL METHODS

A. Method to Explore the Free Energy Surface and Computational Details

At temperatures different of zero, the Gibbs free energy determines the lowest-energy structure,⁵⁰ whereas at temperature zero the enthalpy determines the putative global minimum.^{31,36} A simple analysis of the Gibbs free energy given by $\Delta G = \Delta H - \Delta ST$ deals to a conclusion, in order to minimize the Gibbs free energy we must to maximize the entropy.^{31,36,51} Front the theoretical point of view, and first of all, with the aim to understand molecular properties, at temperatures non-zero, we must know the lowest Gibbs free energy structure or the largest entropy structure, and all structures closest in energy to the lowest energy structure^{31,36} or all high-entropy structures closet in entropy to the largest entropy structure. We must keep in mind that the experiment are performed

at non-zero or finite temperatures. From a very general point of view, it has been shown that the validity of DFT can be extended to finite temperatures by the concept of ensemble DFT.⁵² The search of the global minimum in atomic clusters is complicated task due to the number of possible combinations grows exponentially with the number of atoms leading to a combinatorial explosion problem among others.^{31,36} Despite that is not an easy task, several algorithms to explore globally the potential/free energy surface coupled to a local optimizer generally of any electronic structure package have been successfully employed in a target so far, i.e. AIRSS approach,⁵³ simulated annealing,^{54–59} kick methodology,^{60–71} and genetic algorithms^{31,67,71–76} among many others. Global structure searching at the DFT level are computationally expansive to be applicable to intermediate and large clusters size, as we mentioned early, the number of candidates increase exponentially. In this work we used two-stage procedure to explore efficiently the potential energy surface, in the first stage we perform a global search using a empirical methodology, where Gupta interaction potential were used to describe the Cu-Cu interactions with default parameters taken from references^{77,78} and coupled to Basin Hopping global optimization algorithm implemented in *Python* code and part of global search of GALGOSON code.^{31,36} At the second stage, all the lowest energy structures from the first stage are symmetrized, followed by a DFT optimization that were performed using the Gaussian suite code⁷⁹ employing two exchange-correlation functionals, B3PW91, PBE and two basis set, def2SVP and LANL2DZ, with and without taking into account D3 version of Grimme's dispersion corrections⁸⁰ as implemented in Gaussian 09 code.⁷⁹ The Becke's hybrid three-parameter^{81,82} exchange-correlation functional in combination with the Perdew and Wang GGA functional PW91^{19,83} is known as B3PW91 exchange-correlation functional. The B3PW91 has been employed in other studies of reactivity in copper clusters with good performance,²⁷ whereas, the PBE exchange-correlation functional⁸⁴ has shown good performance in thermochemistry properties.⁸⁵ Regarding the LANL2DZ⁸⁶ basis set, that was used in previous studies of computations of copper-based molecules properties produced result close to experimental values.⁸⁷ Not too long ago, in a previous DFT studies, the def2-SVP⁸⁸ gave good results in the computations of Cu-metal ligand bond lengths.⁸⁹ The true minimum energy structures are validated by the vibrational analysis without imaginary frequency.

B. Thermochemistry Properties

All the thermodynamic properties of an ensemble of molecules can be derived from molecular partition function^{31,36,90,91} so, the molecular partition function contains all thermodynamic information in a similar way that the quantum wavefunction contains all the information about the system.^{31,90} Previous theoretical studies

used the partition function to compute thermodynamic properties of Cu_n clusters (n=2, 150) as a function of temperature and demonstrated that the magic clusters is temperature dependent⁴² Zhen Hua-Li et al.⁴⁰ computed the thermodynamics of unsupported neutral Al_n (2 < n < 65) particles evaluating rovibrational partition functions, they reported that the dominant cluster depends on temperature. and gives an overview of recent progress on the nanothermodynamics of metal nanoparticles.³⁹ Christopher Sutton et al.⁵¹ in framework of atomistic thermodynamics predict the behavior of materials at realistic temperatures. Recently, Buelna-Garcia et al.^{31,36} used the partition function to compute the temperature-dependent relative population and IR spectra of neutral Be₄B₈ and anionic Be₆B₁₁ clusters, also Dzib et al.⁹⁰ employed a similar procedure to compute the reaction rate constants. Other previous theoretical studies computed the temperature-dependent entropic contributions on [Fe(pmea)(NCS)₂] complex.⁹² In this study, the temperature-dependent Gibbs free energy is computed employing the partition function Q given in Equation, 1 under the rigid rotor, harmonic oscillator, Born-Oppenheimer, ideal gas, and a particle-in-a-box approximations. We have to underline that it must take into account the anharmonicity to compare theory with experiment.⁹³

$$Q(T) = \sum_i g_i e^{-\Delta E_i / k_B T} \quad (1)$$

In Eq. 1, g_i is the degeneracy factor, k_B is the Boltzmann constant, T is the temperature, and $-\Delta E_i$ is the total energy of a cluster.^{31,90,94} We employ equations 2 to 5 to compute the internal energy (U), enthalpy (H), and Gibbs energy (G) of the Cu₃₈ cluster at finite temperature. The equations to compute entropy contributions (S) are those employed in a previous work^{31,36,50,90} and any standard thermodynamics textbook.^{94,95}

$$U_0 = \mathcal{E}_0 + ZPE \quad (2)$$

$$U_T = U_0 + (E_{ROT} + E_{TRANS} + E_{vib} + E_{elect}) \quad (3)$$

$$H = U_T + RT \quad (4)$$

$$G = H - TS \quad (5)$$

In Equations above, ZPE is the zero-point energy correction \mathcal{E}_0 is the electronic energy, and $E_{ROT} + E_{TRANS} + E_{VIB} + E_{elect}$ are the contributions to energy due to translation, rotation, vibration and electronic as function of temperature, respectively. To compute the Boltzmann probability of occurrence of one particular neutral Cu₃₈ cluster in an ensemble at thermal equilibrium and at finite temperatures, we employ the probability of

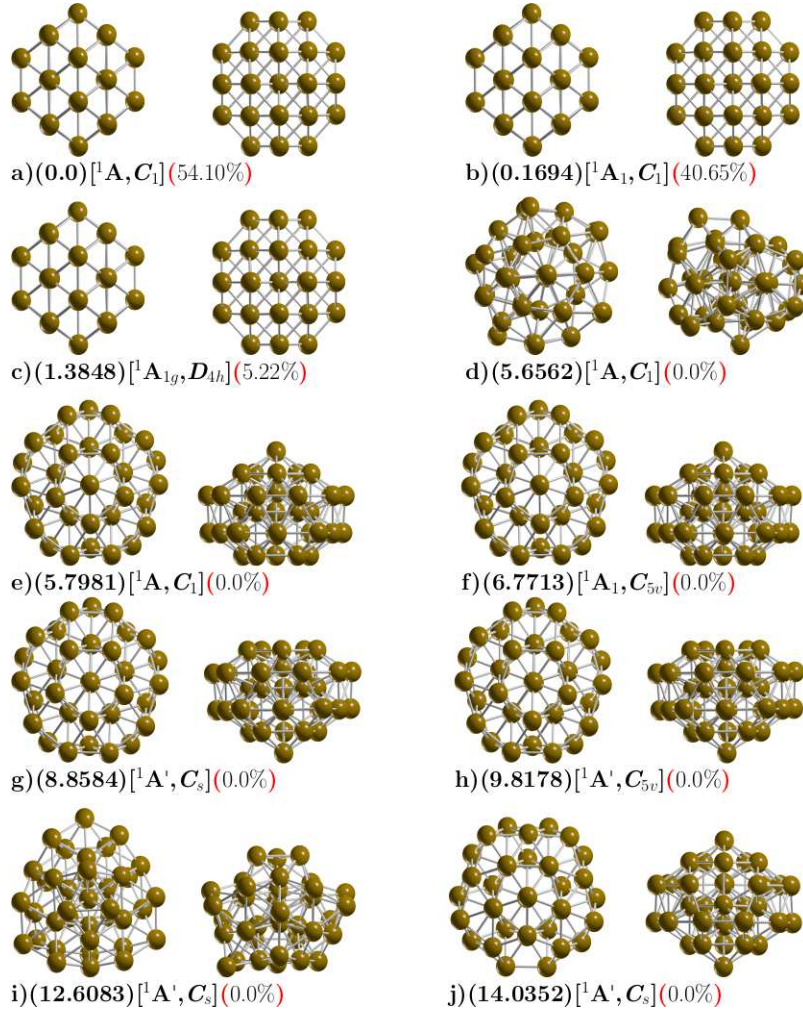


FIG. 1: (Color online) Optimized geometries in front and side views of neutral Cu₃₈ cluster at PBE-GD3/def2-SVP level of theory taking into account D3 version of Grimme's dispersion corrections. The first letter is the isomer label, relative Gibbs free energies in kcal/mol (in round parenthesis) at 298.15 K, electronic group and group symmetry point [in square parenthesis], the probability of occurrence (in red round parenthesis) at 298.15 K, and the yellow-colored spheres represent Cu atoms.

occurrence^{31,35,36,40,40,42,90,96–100} given in Equation 6

$$P_i(T) = \frac{e^{-\beta \Delta G^k}}{\sum e^{-\beta \Delta G^k}}, \quad (6)$$

where $\beta = 1/k_B T$, and k_B is the Boltzmann constant, T is the temperature, and ΔG^k is the Gibbs free energy of the k^{th} isomer. We point out that Gibbs free energies must be corrected considering the symmetry, Buelna-Garcia et al.³⁶ in a previous work shows that the contribution of the rotational entropy to the Gibbs free energy calculated with and without symmetry behave linearly with the temperature and could be significant⁵⁰. Equation 6 is restricted so that the sum of all probabilities of occurrence, at fixed temperature T , $P_i(T)$ is equal to 1

and given by Equation 7

$$\sum_i P_i(T) = 1, \quad (7)$$

In this study, the Boltzmann weighted UV-Vis spectrum at finite temperature is given by Equation 8

$$UV - Vis = \sum_i (UV - Vis)_i \times P_i(T) \quad (8)$$

Where n is the total number of cluster in the ensemble, $UV-Vis_i$ is the UV-Vis of the i^{th} isomer at temperature $T=0$, and $P_i(T)$ is the probability of occurrence of the i isomer given by Equation 6. To compute the probability of occurrence and the spectra we used the Boltzmann-Optics-Full-Ader code (*BOFA*).^{31,35}

III. RESULTS AND DISCUSSION

A. The lowest energy structures and energetics

The ball and stick model shown in Figure 1 depicted the lowest-energy structure and the low-energy structures of neutral Cu₃₈ clusters along with some competing isomers. At B3PW91/def2SVP level of theory and taking into account the dispersion pairwise correction of Grimme (DFT-GD3),⁸⁰ ZPE energy corrections and at room temperature and 1 atmospheric pressure. We found a tetrakaidecahedron as the lowest energy structure which has 14 faces: six equivalent square fcc(100) and eight equivalent hexagons, this shape is obtained when cutting the corners off 3D diamond shape, and it is a fcc-like truncated octahedron (TO). The calculated structure belongs to point group symmetry C₁, electronic ground state ¹A, its lowest IR active vibration frequency is 32.57 cm⁻¹ and is a semiconductor with electronic gap 0.623 eV. It is known that the bulk rare gas crystals have a face centered cubic (FCC) crystalline symmetry.

Previous works on exploration of the potential energy surface of Cu₃₈ cluster using genetic algorithms with Gupta potential often find highly symmetric TO structure,¹⁴ other reported previous work employing *Sutton-Chen* potential with monte Carlo simulation also find TO structure.²⁸ The optimized Cu-Cu bond length is found to be 2.4670 Å which is in good agreement with other reported DFT calculations Cu-Cu dimmer^{101,102} of 2.248, Å and is consistent with the experimental bonding distance Cu-Cu 2.22 Å.¹⁰¹ Our computed diameter of TO structure is 7.8 Å and also is in good agreement of 8 Å reported in previous theoretical DFT calculations.¹⁰² The second structure higher in energy lies at 0.16 kcal/mol at temperature of 298.15 K also is a TO structure with point group symmetry C₁, electronic ground state ¹A, the lowest IR active vibration frequency is 32.13 cm⁻¹, and is a semiconductor with electronic gap 0.623 eV, similarly to that of the putative global minimum. The next structure is slightly higher in energy located at 1.38 kcal/mol also is a TO structure, but with D_{4h} point group symmetry and electronic ground state ¹A_{1g}, and the lowest IR active vibration frequency is 33.44 cm⁻¹. We also explored TO structure, initializing the geometry from the high-symmetries OH and TH and after geometry optimization without constrains, the OH and TH symmetries become C₁ and D_{H4} symmetries. The perfect OH symmetry it could be deformed due to the *Jahn-Teller effect*^{101,102} and would have to be taken into account in the calculation of total energy^{103,104} and the relative population at temperature T could change as consequence in the optical properties.¹⁰⁵ Recently, in one of our previous works, we clarify the origin of Gibbs free energy differences between two similar structures just with different group symmetry, that is due to the rotational entropy, specifically the R T ln(s) factor.³⁶ In this work, the energy difference of 0.16 between the two isomers depicted in Figure 1a with symmetry C₁ and RMSD, the difference is 0.08 and is

due to the Jean teller effect. The structure located at 1.38 kcal/mol above the putative global minimum with D_{4H} symmetry is due to rotational entropy. The next structure, shown in Figure 1d is located at 5.65 kcal/mol above the putative global minimum, with point group symmetry C₁, and electronic ground state ¹A, the lowest IR active vibration frequency is 24.16 cm⁻¹, it is a distorted structure semiconductor with electronic gap of 1.0 eV, the calculated Cu-Cu bond distance is 2.50, Å and the molecular diameter of this structure is 9.1 kcal/mol, slightly larger Cu-Cu bond distance and diameter than the global minimum, this structure possesses the the smallest relative ZPE energy, as shown in Figure, as well as the smallest frequency of the vibrational modes of all isomers. The next two higher energy structures shows in Figure 1(e,f) are located up to 5.8 kcal/mol, an both of them are the incomplete-Mackay icosahedron (IMI) with C₁ and C_{5v} point group symmetries and electronic ground state ¹A and ¹A₁ respectively. For both cases, the molecular diameter is 8.54, Å electronic gap of 0.97 eV eV and the Cu-Cu bonding distance is 2.47 Å. There are other higher energy structures shows in Figure 1(g,h,i,j), these do not contribute to any molecular property in all temperature range. In the Supplementary Information, Figure 8, Appendix D, we depicted the lowest energy structures screening at B3PW91/def2SVP level of theory and without taking into account the atom-pairwise correction of Grimme GD3. The lowest energy structure is IMI structure with point group symmetry C₁ and electronic ground state ¹AH. The molecular diameter is 8.69 Å, slightly larger than those found at TO structure of 7.8, Å the average bond distance is 2.50 Å. At PBE-GD3/Def2SVP level of theory, we found a IMI structure to be the most stable structure whereas at the PBE-GD3/LANL2DZ level of theory we found the TO structure as the putative global minimum energy. The complete description of the structures located at higher energies is in the Supplementary Information. We point out here, for the Cu₃₈ clusters, the order energetically of the isomers and the energy gap among isomers as well as the putative global minimum interchange when we take into account the dispersion interactions. The atomic XYZ coordinates (at B3PW91/def2SVP level of theory) are displayed in Appendix F

B. Energetics

In the computation of energies employing different methods yield different results due to the functional and basis sets and therefore the energetic isomer ordering changes.^{33,36} The comparison of two different exchange-correlation functionals and two basis set and with and without taking into account the dispersion D3 the Grimme are shown in the Table I. The optimizations performed at the B3PW91/PBE-def2TZVP considering the dispersion yield the same type of lowest energy equilibrium geometry and similar energetic isomer ordering when we

TABLE I: The energetic isomer ordering employing B3PW91/Def2TZVP, PBE/Def2TZVP, and PBE/LANL2DZ levels of theory.

Level of theory	Energy	Isomers (energy kcal/mol)								
		i_a	i_b	i_c	i_d	i_e	i_f	i_g	i_h	i_i
B3PW91/Def2TZVP/GD3	ΔG	0.0	0.16	1.38	5.65	5.79	5.81	6.76	8.85	9.81
	$\mathcal{E}_0 + \mathcal{E}_{\text{ZPE}}$	0.0	0.09	0.0	5.01	5.01	5.01	5.01	8.17	
	\mathcal{E}_0	0.05	0.0	0.10	8.76	4.89	4.89	4.88	4.88	
B3PW91/Def2TZVP	ΔG	0.0	0.95	2.0	2.40	2.73	2.91	2.94	3.28	3.32
	$\mathcal{E}_0 + \mathcal{E}_{\text{ZPE}}$	0.0	0.0	2.14	3.29	6.52	3.84	2.14	3.27	3.84
	\mathcal{E}_0	0.0	0.0	2.09	3.27	6.13	3.76	2.09	3.28	3.76
PBE/Def2TZVP/GD3	ΔG	0.0	0.86	0.92	5.02	7.23	7.59	7.81	8.88	12.27
	$\mathcal{E}_0 + \mathcal{E}_{\text{ZPE}}$	0.0	0.89	0.0	8.70	7.94	7.92	8.61	7.94	14.24
	\mathcal{E}_0	0.0	0.90	0.0	9.14	7.92	7.93	8.84	7.94	12.47
PBE/Def2TZVP	ΔG	0.0	0.34	0.92	1.37	1.38	1.77	2.82	5.79	8.70
	$\mathcal{E}_0 + \mathcal{E}_{\text{ZPE}}$	0.0	0.0	0.37	0.41	1.77	1.77	1.77	9.08	15.75
	\mathcal{E}_0	0.0	0.0	0.38	0.39	1.73	1.73	1.74	9.47	9.86
PBE/LANL2DZ/GD3	ΔG	0.0	1.02	3.37	3.46	8.63	9.11	9.59	9.62	9.74
	$\mathcal{E}_0 + \mathcal{E}_{\text{ZPE}}$	2.03	0.0	2.12	2.14	8.31	8.77	8.73	9.34	8.71
	\mathcal{E}_0	1.97	0.0	2.01	2.01	8.08	8.60	8.52	9.12	8.45
PBE/LANL2DZ	ΔG	0.0	2.15	2.87	3.03	3.26	4.31	8.89	9.66	9.85
	$\mathcal{E}_0 + \mathcal{E}_{\text{ZPE}}$	0.97	0.0	1.46	1.38	1.64	1.68	7.98	9.19	9.58
	\mathcal{E}_0	0.86	0.0	1.27	1.11	1.48	1.42	8.03	8.99	9.37

employ the electronic energy with and without ZPE correction energy and Gibbs free energy computed at room temperature. From the energetic point of view, the inclusion of dispersion is more important than the type of functional and basis set, i.e The first line of the Table I show the relative Gibbs free energies computed at the B3PW91-D3/def2TZVP level of theory, the isomer label i_b in the Table I and depicted in Figure 1b is located 0.16 kcal/mol above the putative global minimum whereas the second line of the Table I show the relative Gibbs free energies computed at the B3PW91/def2TZVP level of theory and the isomer i_b in the Table I and depicted in Figure 1b is located 0.95 kcal/mol above the putative global minimum as it is shown in Table I. For isomer i_b , the effect of the dispersion on the energy is decrease the relative Gibbs free energy with respect to the putative global minimum. (from 0.95 to 0.16 kcal/mol). The effect of dispersion, in the case of isomers i_c , is also decrease the relative Gibbs free energy with respect to the putative global minimum from 2.0 to 1.38 kcal/mol whereas for isomer label i_d , the relative Gibbs free energy increase from 2.4 to 5.65 kcal/mol. In summary, the effect of dispersion reduces the Gibbs free energy in the lowest energy structures where the Boltzamnn fac-

tors are difrentes from zero. A overall comparison of free energies computed with functional B3PW91, second line of the Table I, and PBE in four line in the Table I, versus free energies computed with functional PBE, four line of the Table I, and PBE in four line in the Table I, shows a reduction in the relative Gibbs free energies when the PBE functional is employed. For the case of the basis set the LANL2DZ increase the relative Gibbs free energy in the low energy isomers as it is shows a comparison of line 6 of Table I versus line 1 of Table I.

C. Relative stability

The probability of finding the TO structure with C_1 symmetry at B3PW91/def2-SVP level of theory is depicted in black-solid line in panel (a) of Figure 1(4). It strongly dominates from 0 to 300 K, thus all the molecular properties are due only to this structure. From slightly before 300 K, it start to decay exponentially and almost disappear at 900 K, at the same time, the probability of finding the amorphous structure with point group symmetry C_1 , is depicted in violet-solid line in Figure 2(a), it start to grow exponentially and become

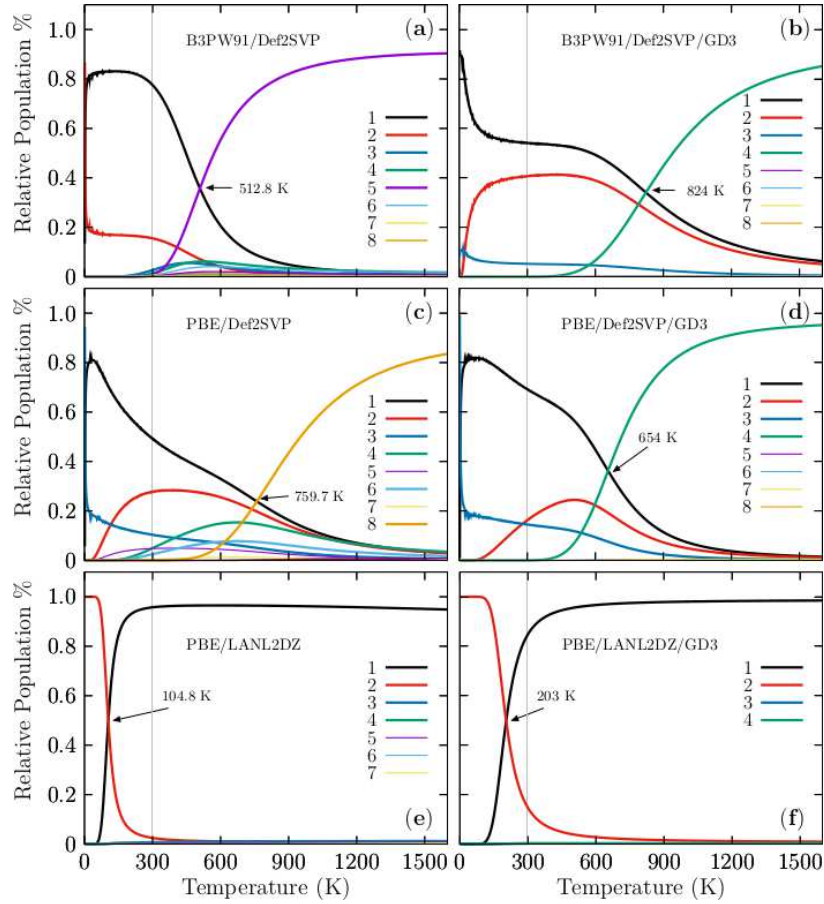


FIG. 2: (Color online) The relative stability/population or probabilities of occurrence for temperatures ranging from 20 to 1500 K at three different levels of theory B3PW91/def2-SVP, PBE/def2-SVP and PBE/LANL2DZ with and without D3 Grimme dispersion. The effect of dispersion on the solid-solid transformation point in temperature scale and in all cases is large for Cu₃₈ cluster. At hot temperatures, in all cases the dominant structure is a amorphous geometry depicted in Figure 1(4) whereas at cold temperatures, the dominant structure can change from TO to inverted incomplete-Mackay icosahedron (IIMI) structures. The TO structure depicted in Figure 1(1) is the strong dominant structure at cold temperatures at B3PW91-GD3/def2-SVP level of theory.

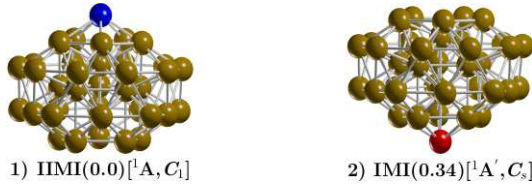


FIG. 3: We depicted the inverted incomplete-Mackay icosahedron (IIMI) label 1 with symmetry C₁ and the incomplete-Mackay icosahedron (IMI) label 2 with symmetry C_s and located 0.34 kcal/mol energy above the putative minimum global at 298.15 K. The yellow, red and blue colored spheres represent copper atoms. The IIMI structure is the result of interchanging the red Cu atom depicted in the IMI structure to the position of blue atom in the IIMI structure. The IMI structure was reported in reference⁶ as the low-energy structure. The HOMO-LUMO gap of the IMI structure is 0.24 eV (0.356 eV reported by previous DFT studies⁶) whereas for the HOMO-LUMO gap for IIMI structure is 0.30 eV, suggesting why the IIMI structure is energetically more stable.

dominate at temperature above 512.8 K and at 900 K it become strongly dominate. At solid-solid transition temperature of 512.8 K the TO and the amorphous structure

co-exist. The effect of dispersion can be appreciated in panel (b) of Figure 2. The relative population is computed at B3PW91-G3/def2-SVP level of theory. The ef-

fect of the dispersion is dramatic, the solid-solid transformation point is shifted from 512.8 to 824 K, an increase of 160% and from the panel (b) one can see that the molecular properties below 600 K, are due to only the TO structure. Slightly before 600 K, The probability of finding the amorphous structure, depicted in green-solid line in panel (b), start to grow up exponentially and at temperature of 824 K the TO and amorphous structure co-exist. Whereas a temperature of 600 K the probability of find the TO structure start do decay exponentially and at 900 K its value still around 20%. The probabilities of occurrence at the PBE/def2-SVP level of theory of a particular Cu₃₈ isomer are displayed in panel (c) of Figure 2. The dominant putative global minimum structure at T=0, is the inverted incomplete-Mackay icosahedron (IIMI) structure depicted in Figure 3a with C₁ symmetry and its probrobability of finding it is depicted as a black solid line in panel (c) of Figure 2. Its probability decays almost linearly until 1000 K where it almost disappears. At temperature of 759.7 K, the solid-solid transformation point, the IIMI structure co-exist with an amorphous structure. The probability of finding the amorphous structure start to grew up at 600 K, and above of solid-solid transformation point, it start to strongly dominate as putative global minimum. Where the probability of finding the IMI structure is depicted in red-solid line on panel (c) of Figure 2, the largest probability is 30% at room temperature. Interesting, the probabilities of IIMI and IMI structures does not cross at cold temperature. Zhang et al.⁶ reported that IMI structure could be highly competitive at finite temperatures, but our findings shows that the amorphous structure with C₁ symmetry is highly dominant at hot temperatures, whereas the IIMI structure is highly dominant at cold temperatures.

For ease comparison, the Figure 3 display the IIMI and the IMI structures side by side. At cold and the IIMI structure dominate. The effects of dispersion is shift the solid-solid transformation point to lower temperatures from 759.7 K to 654 K as one can see in panel (d) Figure 2. The probability of finding the IIMI structure as a function of temperature is depicted in black solid-line and it decays approximately linearly from 50 to 500 K, after that it decays exponentially until 900 K where it disappears. At around 400 K, the probability of finding the amorphous structure, depicted in green solid-line in panel (d) of Figure 2, start to grow up in exponential way, and at temperature of 654 K it co-exit with the IIMI structure. Above 654 K, the amorphous structure becomes energetically favorable.

D. IR spectra at finite temperature

The properties observed in a molecule are statistical averages over the ensemble of geometrical conformations or isomers accessible to the cluster, so the molecular properties are governed by the Boltzmann distributions

of isomers that can change significantly with the temperature primary due to entropic effects.^{31,36,40} The major contributions to the entropy are the many soft vibrational modes that the clusters possesses. The IR spectrum is related to vibrations or rotations that alter the dipole moment, and it will happen in molecules that have a dipole moment. Also, the IR spectrum is related to the curvature of the potential curve versus interatomic distances. Complete information about molecular vibrations allows us to analyze catalytic chemical reactions.^{106–108} IR spectra are used to identify functional groups and chemical bond information. However, assigning IR bands to vibrational molecular modes in the measured spectra can be difficult and requires DFT calculations; as we mentioned earlier, the temperature is not considered in these computations and discrepancies between experimental and computed IR spectra can result from finite temperature, anharmonic effects, and multi-photon nature of experiments, whereas IR computations assume single-photon processes.^{31,36} The IR spectra of isolated metal clusters in the gas phase for vanadium cluster cations as well as for neutral and cationic niobium clusters were measured.¹⁰⁹ Even though Cu clusters are important in catalysis and were the first clusters experimentally produced,¹¹⁰ the available structural information is limited to study photoelectron spectroscopy for anions, mass spectrometry, and photodissociation spectra in the visible range.¹¹¹ Reciently, Lushchikova et al.¹¹¹ determine the structure of small cationic copper clusters based on a combination of IR spectroscopy of Cu_n⁺-Ar_m complexes and DFT calculations. In this work, the IR spectra of isomers computations were carried out using the Gaussian package under harmonic approximation at level of theory PBPW91-D3¹¹²/def2TZVP and full width at half maximum (FWHM) of 8 cm⁻¹ taking into account the dispersion of Grimme D3 as implemented in Gaussian code. Negative frequencies were checked in all calculations to ensure that there were not transitions states. The computed frequencies were scaled by 0.98 to estimate the observed frequencies. Here, the total IR spectrum is computed as a weighted Boltzmann sum of the single IR spectrum of each isomer of the distribution at finite temperature^{31,36,113,114} given by Equation 8 and the probabilities of occurrence displayed in Figure 2. To our knowledge, there are a few theoretical studies on IR spectra of noble metal clusters computed considering a weighted sum of the IR spectra of isomers.¹¹⁴ Computed weighted Boltzmann IR spectra of Cu₃₈ clusters at different temperatures are shown in Figure 6, Appendix B. Notice that the transition metal clusters are very stable, and its vibrational frequencies are found below 400 cm⁻¹¹¹⁵ in good agreement with our computed spectra displayed in Figure 6, Appendix B.

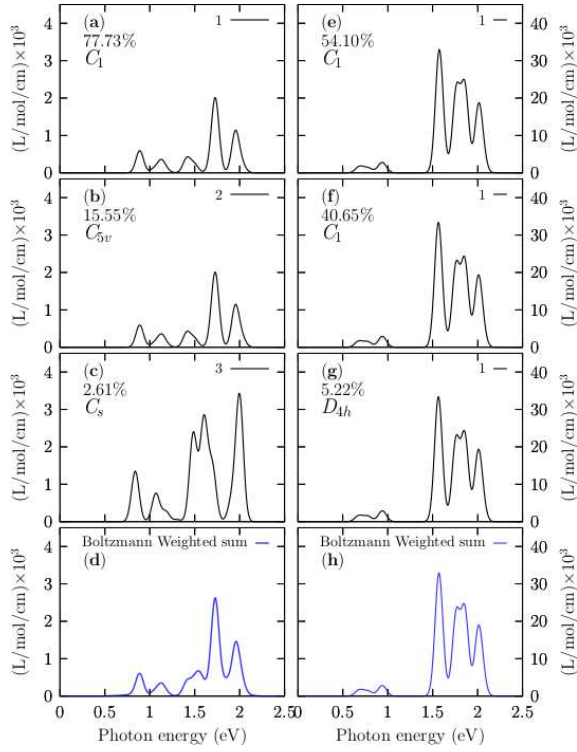


FIG. 4: The dependent temperature UV-visible Boltzmann-spectra-weighted at room temperature of the neutral Cu₃₈ cluster are shown in panels (e) to (g) with Grimme's dispersion GD3 (without GD3 panels (a) to (d)). The computed UV-visible spectrum of each isomer is multiplied by their corresponding Boltzmann weight at finite temperature; then, they are summed together to produce a final Boltzmann-weighted UV spectrum. Each spectrum of each isomer were computed employing time-dependent density functional theory (TD-DFT) as implemented in Gaussian code at the CAM-B3LYP/def2-SVP level of theory employing geometries optimized at B3PW91-D3/def2-SVP.

E. UV-Visible spectra at finite temperature

The optical properties are a source of atomic structural information, and their electronic structure determines them.¹¹⁶ In this paper the TD-DFT was used to compute the optical absorption spectra in the UV-visible range $0.5 < \hbar\omega < 2.5$ eV for the Cu₃₈ cluster. We employ the CAM-B3LYP functional, Def2-TZVP basis set, and 50 singlets and 50 triplets states. The transition metals clusters allow us to study the influence of the **d** electrons on the optical properties; it is known that the **d** electrons strongly influence the surface plasmon response.¹¹³

We show in Figure 4 the UV-spectra for the Cu₃₈ cluster with and without the Grimme's dispersion D3. To take into account the effects of temperature on the UV-visible spectra. We consider that the UV-visible spectrum of a molecular ensemble is a weighted sum of all the individual contributions of each isomer that forms the ensemble. In panel labeled (e) is displayed the UV spectra

considering the Grimme's dispersion GD3 and for the lowest energy structure with symmetry C₁; this structure contribute with 54% to the total Boltzmann spectrum. In panel (f) is displayed the UV-visible for the low-energy structure located at 0.16 kcal/mol at room temperature and above the putative global minimum with C₁ symmetry, and this contributes to 40% to the Boltzmann spectrum. In panel (g) is displayed the UV-visible for the low-energy structure located at 1.38 kcal/mol at room temperature and above the putative global minimum with D_{4h} symmetry, and this contributes to 5.22% to the Boltzmann spectrum. In panel (h) is displayed the Boltzmann weighted UV-Visible spectrum at room temperature. Notice that all absorption spectra, (g) to (h), are similar; The Boltzmann weighted UV-Visible spectrum presented in Figure 4, panel (h) is composed of three peaks located between 1.5 to 2 eV and smaller intensity peaks located at 0.5 and 1.0 eV. The most significant absorption peak is located at 1.6 eV. Our computations show five absorption peaks of the UV-visible spectrum starting at 0.5 eV and finishing at 2.5 eV. Notice that the total optical spectrum is due only to the putative global minimum; despite the number of isomers growing exponentially, the main contribution to the optical properties comes from those low energy structures very close to the global minimum where weights Boltzmann factors temperature dependents are different from zero. Interestingly, the second low-energy structure located at 0.16 kcal/mol (room temperature) above the putative lowest energy structure screen or blocked the contributions to the Boltzmann optical spectrum of the other structures. In this paper, we called those structures as *shielding structures*. In Figure 4, panels (a) to (d) are displayed the optical absorption spectra in the UV-visible range computed with structures optimized without the Grimme's dispersion D3. Notice the effects of dispersion on UV-visible spectra is introduced by the change of the relative population when the optimizations are computed without, and with dispersion, e.g., the contribution, to the Boltzmann weighted UV-Visible spectrum, of the lowest energy structure computed without Grimme's dispersion D3 is 77% meanwhile, the contribution is 54% when an optimized structure is computed with Grimme's dispersion D3. The complete evolution of the Boltzmann weighted UV-Visible spectra for temperatures ranging from 10 to 1500 K is displayed in Figure 7, Appendix C.

F. Molecular Dynamics

We performed Born-Oppenheimer molecular dynamics (MD) of the Cu₃₈ cluster employing the deMon2K program¹¹⁷ (deMon2k v. 6.01, Cinvestav, Mexico City, Mexico, 2011) at temperature of 600 K, aiming to gain insight into the dynamical behavior of the Cu₃₈ cluster. The MD started from global putative minimum structure. The simulation time

was 25 ps with a step size of 1 fs. All computations were performed under scheme of ADFT,¹¹⁸ and for the basis set we employed the double zeta plus valence polarization (DZVP) all-electron basis. We employed the Nosé-Hoover thermostat to fix the temperature and the linear and angular momenta of the cluster Cu₃₈ were initialized to zero and conserved.

IV. CONCLUSIONS

For the first time, to our knowledge and from our results, we proposed the inverted incomplete-Mackay icosahedron (IIMI) with symmetry C₁ as low-energy structure than the incomplete-Mackay icosahedron (IMI) with symmetry C_s and located 0.34 kcal/mol energy above the putative minimum global at 298.15 K. The yellow, the IIMI structure is the result of interchanging the red Cu atom depicted in the IMI structure to the position of blue atom in the IIMI structure. The IMI structure was reported in reference⁶ as the low-energy structure. The HOMO-LUMO gap of the IMI structure is 0.24 eV (0.356 eV reported by previous DFT studies⁶) whereas for the HOMO-LUMO gap for IIMI structure is 0.30 eV, suggesting why the IIMI structure is energetically more stable. We computed the effect of symmetry on the Boltzmann populations on Cu₃₈ clusters. In spite that the number of isomers grows exponentially, the main contribution to the optical properties comes from those low energy structures very close to the global minimum where weights Boltzmann factors temperature dependents are different from zero. We performed an unbiased global search for minimum energy Cu₃₈ clusters structures using a two-stage strategy. First a global search using a semi empirical methodology, followed by a density functional theory optimization of the best structures from the first stage was done at different levels of theory. The temperature and entropic effects cause several competing structures because energy separation between isomers on the free energy surface is small and changes the dominant structure, so probably a mixture of isomers interconverted at temperature finite. Those energetically competing structures provide a different percentage of the entire IR spectrum. On the other hand, those higher energy structures with significant energy separation among isomers on the potential energy surface do not contribute to the entire IR spectrum. Despite that, the number of isomers grows exponentially. The main contribution to the molecular properties comes from those low-energy structures very close to the global minimum, where weight's Boltzmann factors temperature dependents are different from zero.

(depends strongly on the energy separation, if the energy separation is significant, the IR spectrum going to be rigid, not changes) A motif is dominant in cold conditions, whereas the other motif is dominant in other hot conditions; additionally, the level of theory is decisive in the computations of TSS point dependent-temperature Our computations clearly show (relative population) that the low-symmetry isomers become more stable at high temperatures due to the entropic effect and the fact that energy states of molecules follow Boltzmann distribution in all six different levels of theory. Our unbiased global search on the free energy surface show that there is an amorphous structure that strongly dominate at hot temperatures, as far as we know this is a novel putative global minimum at hot temperatures. As immediate work is the computations of the relative populations at high level of theory and compute the T_1 diagnostic to determine that the computed DFT energies are not properly described by a single reference method or contain a multireference character. So, further studies needed to be done.

V. ACKNOWLEDGMENTS

C. E. B.-G. thanks Conacyt for the Ph.D. scholarship (860052). E. P.-S. thanks Conacyt for the Ph.D. scholarship (1008864). We are grateful Universidad Politécnica de Tapachula (UPTap) for granting us access to their clusters and computational support. We are also grateful to the computational chemistry laboratory and ICEME research group at UPTap for providing computational resources, *ELBAKYAN*, and *PAKAL* supercomputers.

VI. CONFLICTS OF INTEREST

The authors declare no conflict of interest.

VII. FUNDING

This research received no external funding.

VIII. ABBREVIATIONS

The following abbreviations are used in this manuscript:

Density Functional Theory (DFT)
Zero-Point Energy (ZPE)

* email:germtzguajardo@uaz.edu.mx

† email:sollebac@gmail.com, jose.cabellos@uptapachula.edu.mx

¹ J. P. Wilcoxon and B. L. Abrams. Synthesis, structure and properties of metal nanoclusters. *Chem. Soc. Rev.*,

35:1162–1194, 2006.

² Riccardo Ferrando, Julius Jellinek, and Roy L. Johnston. Nanoalloys: From theory to applications of alloy clusters and nanoparticles. *Chemical Reviews*, 108(3):845–

- 910, 2008.
- ³ Gajendra Kumar Inwati, Yashvant Rao, and Man Singh. Thermodynamically induced in situ and tunable cu plasmonic behaviour. *Scientific Reports*, 8(1):3006, Feb 2018.
- ⁴ Ammu Mathew and Thalappil Pradeep. Noble metal clusters: Applications in energy, environment, and biology. *Particle & Particle Systems Characterization*, 31(10):1017–1053, 2014.
- ⁵ Paulrajpillai Lourdu Xavier, Kamalesh Chaudhari, Ananya Baksi, and Thalappil Pradeep. Protein-protected luminescent noble metal quantum clusters: an emerging trend in atomic cluster nanoscience. *Nano reviews*, 3:10.3402/nano.v3i0.14767, 2012.
- ⁶ Chuanchuan Zhang, Haiming Duan, Xin Lv, Biaobing Cao, Ablat Abliz, Zhaofeng Wu, and Mengqiu Long. Static and dynamical isomerization of Cu₃₈ cluster. *Scientific Reports*, 9(1):7564, May 2019.
- ⁷ Peisheng Liu, Hao Wang, Xiaoming Li, Muchen Rui, and Haibo Zeng. Localized surface plasmon resonance of Cu nanoparticles by laser ablation in liquid media. *RSC Adv.*, 5:79738–79745, 2015.
- ⁸ Puru Jena and A. W. Castleman. Clusters: A bridge across the disciplines of physics and chemistry. *Proceedings of the National Academy of Sciences*, 103(28):10560–10569, 2006.
- ⁹ Dung T. Tran and Roy L. Johnston. Theoretical study of Cu_{38-n}Au_n clusters using a combined empirical potential-density functional approach. *Phys. Chem. Chem. Phys.*, 11:10340–10349, 2009.
- ¹⁰ Francesca Baletto, Arnaldo Rapallo, Giulia Rossi, and Riccardo Ferrando. Dynamical effects in the formation of magic cluster structures. *Phys. Rev. B*, 69:235421, Jun 2004.
- ¹¹ Walt A. de Heer. The physics of simple metal clusters: experimental aspects and simple models. *Rev. Mod. Phys.*, 65:611–676, Jul 1993.
- ¹² Jonathan P. K. Doye and David J. Wales. Global minima for transition metal clusters described by Sutton-Chen potentials. *New J. Chem.*, 22:733–744, 1998.
- ¹³ C. L. Pettiette, S. H. Yang, M. J. Craycraft, J. Conceicao, R. T. Laaksonen, O. Cheshnovsky, and R. E. Smalley. Ultraviolet photoelectron spectroscopy of copper clusters. *The Journal of Chemical Physics*, 88(9):5377–5382, 1988.
- ¹⁴ O. Kostko, N. Morgner, M. Astruc Hoffmann, and B. von Issendorff. Photoelectron spectra of Na_n- and Cu_n- with n = 20–40: observation of surprising similarities. *The European Physical Journal D - Atomic, Molecular, Optical and Plasma Physics*, 34(1):133–137, Jul 2005.
- ¹⁵ Nobuhisa Fujima and Tsuyoshi Yamaguchi. Magnetic anomaly and shell structure of electronic states of nickel microclusters. *Journal of the Physical Society of Japan*, 58(9):3290–3297, 1989.
- ¹⁶ Christopher D. Taylor, Matthew Neurock, and John R. Scully. First-principles investigation of the fundamental corrosion properties of a model Cu₃₈ nanoparticle and the (111), (113) surfaces. *Journal of The Electrochemical Society*, 155(8):C407, 2008.
- ¹⁷ Dabin Qi, Xudong Luo, Jun Yao, Xiaojun Lu, and Zhan Zhang. Computational study of reverse water gas shift reaction on Cu₃₈ cluster model and cu slab model. *Journal of Theoretical and Computational Chemistry*, 19(02):2050008, 2020.
- ¹⁸ Nozomi Takagi, Kazuya Ishimura, Masafuyu Matsui, Ryōichi Fukuda, Masahiro Ehara, and Shigeyoshi Sakaki. Core-shell versus other structures in binary Cu₃₈-nMn nanoclusters (M = Ru, Rh, Pd, Ag, Os, Ir, Pt, and Au; n = 1, 2, and 6): Theoretical insight into determining factors. *The Journal of Physical Chemistry C*, 121(19):10514–10528, 2017.
- ¹⁹ John P. Perdew, J. A. Chevary, S. H. Vosko, Koblar A. Jackson, Mark R. Pederson, D. J. Singh, and Carlos Fiolhais. Atoms, molecules, solids, and surfaces: Applications of the generalized gradient approximation for exchange and correlation. *Phys. Rev. B*, 46:6671–6687, Sep 1992.
- ²⁰ Masahiro Itoh, Vijay Kumar, Tadafumi Adschiri, and Yoshiyuki Kawazoe. Comprehensive study of sodium, copper, and silver clusters over a wide range of sizes 2 < n < 75. *The Journal of Chemical Physics*, 131(17):174510, 2009.
- ²¹ I. A. Hijazi and Y. H. Park. Structure of pure metallic nanoclusters: Monte carlo simulation and ab initio study. *The European Physical Journal D*, 59(2):215–221, Aug 2010.
- ²² V. G. Grigoryan, D. Alamanova, and M. Springborg. Structure and energetics of nickel, copper, and gold clusters. *The European Physical Journal D - Atomic, Molecular, Optical and Plasma Physics*, 34(1):187–190, Jul 2005.
- ²³ Şakir Erkoç and Riad Shaltaf. Monte carlo computer simulation of copper clusters. *Phys. Rev. A*, 60:3053–3057, Oct 1999.
- ²⁴ Şakir Erkoç. An empirical many-body potential energy function constructed from pair-interactions. *Zeitschrift für Physik D Atoms, Molecules and Clusters*, 32(3):257–260, Sep 1994.
- ²⁵ Valeri G. Grigoryan, Denitsa Alamanova, and Michael Springborg. Structure and energetics of Cu_N clusters with (2 < N < 150): An embedded-atom-method study. *Phys. Rev. B*, 73:115415, Mar 2006.
- ²⁶ Bo Zhao, Riguang Zhang, Zaixing Huang, and Baojun Wang. Effect of the size of Cu clusters on selectivity and activity of acetylene selective hydrogenation. *Applied Catalysis A: General*, 546:111–121, 2017.
- ²⁷ Estefanía Fernández, Mercedes Boronat, and Avelino Corma. Trends in the reactivity of molecular O₂ with copper clusters: Influence of size and shape. *The Journal of Physical Chemistry C*, 119(34):19832–19846, 2015.
- ²⁸ Sarah Darby, Thomas V. Mortimer-Jones, Roy L. Johnston, and Christopher Roberts. Theoretical study of Cu-Au nanoalloy clusters using a genetic algorithm. *The Journal of Chemical Physics*, 116(4):1536–1550, 2002.
- ²⁹ S. Núñez and R. L. Johnston. Structures and chemical ordering of small Cu-Ag clusters. *The Journal of Physical Chemistry C*, 114(31):13255–13266, 2010.
- ³⁰ Young Ho Park and Iyad A. Hijazi. Critical size of transitional copper clusters for ground state structure determination: empirical and ab initio study. *Molecular Simulation*, 38(3):241–247, 2012.
- ³¹ Carlos Emiliano Buelna-Garcia, José Luis Cabellos, Jesus Manuel Quiroz-Castillo, Gerardo Martinez-Guajardo, Cesar Castillo-Quevedo, Aned de Leon-Flores, Gilberto Anzueto-Sánchez, and Martha Fabiola Martin-del Campo-Solis. Exploration of free energy surface and thermal effects on relative population and infrared spectrum of the Be₆B₁₁⁻ fluxional cluster. *Materials*, 14(1), 2021.
- ³² Cesar Castillo-Quevedo, Carlos Emiliano Buelna-Garcia, Edgar Paredes-Sotelo, Eduardo Robles-Chaparro, Edgar Zamora-Gonzalez, Martha Fabiola Martin-del Campo-

- Solis, Jesus Manuel Quiroz-Castillo, Teresa del Castillo-Castro, Gerardo Martínez-Guajardo, Aned de Leon-Flores, Manuel Cortez-Valadez, Filiberto Ortiz-Chi, Tullio Gaxiola, Santos Jesus Castillo, Alejandro Vásquez-Espinal, Sudip Pan, and Jose Luis Cabellos. Effects of temperature on enantiomerization energy and distribution of isomers in the chiral Cu₁₃ cluster. *Molecules*, 26(18), 2021.
- ³³ E. de la Puente, A. Aguado, A. Ayuela, and J. M. López. Structural and electronic properties of small neutral (MgO)_n clusters. *Phys. Rev. B*, 56:7607–7614, Sep 1997.
- ³⁴ Nicola Marzari, David Vanderbilt, and M. C. Payne. Ensemble density-functional theory for ab initio molecular dynamics of metals and finite-temperature insulators. *Phys. Rev. Lett.*, 79:1337–1340, Aug 1997.
- ³⁵ Ana María Mendoza-Wilson, René Renato Balandrán-Qintana, and José Luis Cabellos. Thermochemical behavior of sorghum procyanidin trimers with C4-C8 and C4-C6 interflavan bonds in the reaction with superoxide anion radical and H₂O₂-forming NADH-oxidase flavoenzyme. *Computational and Theoretical Chemistry*, 1186:112912, 2020.
- ³⁶ Carlos Emiliano Buelna-García, Eduardo Robles-Chaparro, Tristan Parra-Arellano, Jesus Manuel Quiroz-Castillo, Teresa del Castillo-Castro, Gerardo Martínez-Guajardo, Cesar Castillo-Quevedo, Aned de León-Flores, Gilberto Anzueto-Sánchez, Martha Fabiola Martin-del Campo-Solis, Ana Maria Mendoza-Wilson, Alejandro Vásquez-Espinal, and Jose Luis Cabellos. Theoretical prediction of structures, vibrational circular dichroism, and infrared spectra of chiral Be₄B₈ cluster at different temperatures. *Molecules*, 26(13), 2021.
- ³⁷ L. V. Redel, Yu. Ya. Gafner, and S. L. Gafner. Role of magic numbers in structure formation in small silver nanoclusters. *Physics of the Solid State*, 57(10):2117–2125, Oct 2015.
- ³⁸ Terrell L. Hill. Thermodynamics of small systems. *The Journal of Chemical Physics*, 36(12):3182–3197, 1962.
- ³⁹ Zhen Hua Li and Donald G. Truhlar. Nanothermodynamics of metal nanoparticles. *Chem. Sci.*, 5:2605–2624, 2014.
- ⁴⁰ Zhen Hua Li, Ahren W. Jasper, and Donald G. Truhlar. Structures, rugged energetic landscapes, and nanothermodynamics of Al_n (2≤n≤65) particles. *Journal of the American Chemical Society*, 129(48):14899–14910, 2007. PMID: 17994736.
- ⁴¹ Francesca Baletto and Riccardo Ferrando. Structural properties of nanoclusters: Energetic, thermodynamic, and kinetic effects. *Rev. Mod. Phys.*, 77:371–423, May 2005.
- ⁴² Valeri G. Grigoryan and Michael Springborg. Temperature and isomeric effects in nanoclusters. *Phys. Chem. Chem. Phys.*, 21:5646–5654, 2019.
- ⁴³ M. Bixon and Joshua Jortner. Energetic and thermodynamic size effects in molecular clusters. *The Journal of Chemical Physics*, 91(3):1631–1642, 1989.
- ⁴⁴ Florent Calvo. Thermodynamics of nanoalloys. *Phys. Chem. Chem. Phys.*, 17:27922–27939, 2015.
- ⁴⁵ David J. Wales. Structure, dynamics, and thermodynamics of clusters: Tales from topographic potential surfaces. *Science*, 271(5251):925–929, 1996.
- ⁴⁶ Gerardo Martínez-Guajardo, Jose Luis Cabellos, Andres Díaz-Celaya, Sudip Pan, Rafael Islas, Pratim K. Chattaraj, Thomas Heine, and Gabriel Merino. Dynamical behavior of borospherene: A nanobubble. *Sci. Report*, 22:11287–11297, June 2015.
- ⁴⁷ Koichi Ohno and Satoshi Maeda. Global reaction route mapping on potential energy surfaces of formaldehyde, formic acid, and their metal-substituted analogues. *The Journal of Physical Chemistry A*, 110(28):8933–8941, 2006. PMID: 16836457.
- ⁴⁸ Carlos Emiliano Buelna-García, Cesar Castillo-Quevedo, Edgar Paredes-Sotelo, Gerardo Martínez-Guajardo, and Jose Luis Cabellos. Boltzmann populations of the fluxional Be₆B₁₁⁻ and chiral Be₄B₈ clusters at finite temperatures computed by DFT and statistical thermodynamics. *IntechOpen: Doi:10.5772/intechopen.100771*, 2021.
- ⁴⁹ Uzi Even, Narda Ben-Horin, and Joshua Jortner. Multistate isomerization of size-selected clusters. *Phys. Rev. Lett.*, 62:140–143, Jan 1989.
- ⁵⁰ Carlos Emiliano Buelna-García, Cesar Castillo-Quevedo, Jesus Manuel Quiroz-Castillo, Edgar Paredes-Sotelo, Manuel Cortez-Valadez, Martha Fabiola Martin-del Campo-Solis, Tzarara López-Luke, Marycarmen Utrilla-Vázquez, Ana Maria Mendoza-Wilson, Peter L. Rodríguez-Kessler, Alejandro Vazquez-Espinal, Sudip Pan, Aned de Leon-Flores, Jhonny Robert Mis-May, Adán R. Rodríguez-Domínguez, Gerardo Martínez-Guajardo, and Jose Luis Cabellos. Relative populations and IR spectra of Cu₃₈ cluster at finite temperature based on DFT and statistical thermodynamics calculations. *Frontiers in Chemistry*, 10, 2022.
- ⁵¹ Christopher Sutton and Sergey V. Levchenko. First-principles atomistic thermodynamics and configurational entropy. *Frontiers in Chemistry*, 8:757, 2020.
- ⁵² Peter Kratzer and Jorg Neugebauer. The basics of electronic structure theory for periodic systems. *Frontiers in Chemistry*, 7, 2019.
- ⁵³ Chris J Pickard and R J Needs. Ab initio random structure searching. *Journal of Physics: Condensed Matter*, 23(5):053201, jan 2011.
- ⁵⁴ S. Kirkpatrick, C. D. Gelatt, and M. P. Vecchi. Optimization by simulated annealing. *Science*, 220(4598):671–680, 1983.
- ⁵⁵ Nicholas Metropolis, Arianna W. Rosenbluth, Marshall N. Rosenbluth, Augusta H. Teller, and Edward Teller. Equation of state calculations by fast computing machines. *J. Chem. Phys.*, 21(6):1087–1092, 1953.
- ⁵⁶ Y. Xiang and X. G. Gong. Efficiency of generalized simulated annealing. *Phys. Rev. E*, 62:4473–4476, Sep 2000.
- ⁵⁷ Yang Xiang, Sylvain Gubian, Brian Suomela, and Julia Hoeng. Generalized simulated annealing for global optimization: the GenSA package for R. *The R Journal*, 5(1):13–29, June 2013.
- ⁵⁸ D.G. Vlachos, L.D. Schmidt, and R. Aris. Comparison of small metal clusters: Ni, Pd, Pt, Cu, Ag, Au. *Z. Phys. D Atom Mol. Cl.*, 26(1):156–158, 1993.
- ⁵⁹ V. Granville, M. Krivanek, and J.-P. Rasson. Simulated annealing: a proof of convergence. *IEEE Trans. Pattern Anal. Mach. Intell.*, 16(6):652–656, 1994.
- ⁶⁰ Sudip Pan, Diego Moreno, Jose Luis Cabellos, Jonathan Romero, Andres Reyes, Gabriel Merino, and Pratim K. Chattaraj. In quest of strong Be-Ng bonds among the neutral Ng-Be complexes. *The Journal of Physical Chemistry A*, 118(2):487–494, 2014. PMID: 24199587.
- ⁶¹ Zhong-hua Cui, Yi-hong Ding, Jose Luis Cabellos, Edisson Osorio, Rafael Islas, Albeiro Restrepo, and Gabriel

- Merino. Planar tetracoordinate carbons with a double bond in CaI_3E clusters. *Phys. Chem. Chem. Phys.*, 17:8769–8775, 2015.
- ⁶² Alba Vargas-Caamal, Sudip Pan, Filiberto Ortiz-Chi, Jose Luis Cabellos, Roberto A. Boto, Julia Contreras-Garcia, Albeiro Restrepo, Pratim K. Chattaraj, and Gabriel Merino. How strong are the metallocene–metallocene interactions? cases of ferrocene, ruthenocene, and osmocene. *Phys. Chem. Chem. Phys.*, 18:550–556, 2016.
- ⁶³ Alba Vargas-Caamal, Jose Luis Cabellos, Filiberto Ortiz-Chi, Henry S. Rzepa, Albeiro Restrepo, and Gabriel Merino. How many water molecules does it take to dissociate HCl? *Chemistry – A European Journal*, 22(8):2812–2818, 2016.
- ⁶⁴ Zhong-hua Cui, Valentin Vassilev-Galindo, Jose Luis Cabellos, Edison Osorio, Mesías Orozco, Sudip Pan, Yi-hong Ding, and Gabriel Merino. Planar pentacoordinate carbon atoms embedded in a metallocene framework. *Chem. Commun.*, 53:138–141, 2017.
- ⁶⁵ Alba Vargas-Caamal, Filiberto Ortiz-Chi, Diego Moreno, Albeiro Restrepo, Gabriel Merino, and Jose Luis Cabellos. The rich and complex potential energy surface of the ethanol dimer. *Theoretical Chemistry Accounts*, 134(2):16, 2015.
- ⁶⁶ Elizabeth Flórez, Nancy Acelas, César Ibargüen, Sukanta Mondal, Jose Luis Cabellos, Gabriel Merino, and Albeiro Restrepo. Microsolvation of NO_3^- : structural exploration and bonding analysis. *RSC Adv.*, 6:71913–71923, 2016.
- ⁶⁷ Estefanía Ravell, Said Jalife, Jorge Barroso, Mesias Orozco-Ic, Gerardo Hernandez-Juarez, Filiberto Ortiz-Chi, Sudip Pan, Jose Luis Cabellos, and Gabriel Merino. Structure and bonding in CE_5^- ($\text{E}=\text{Al-Tl}$) clusters: Planar tetracoordinate carbon versus pentacoordinate carbon. *Chemistry - An Asian Journal*, 13(11):1467–1473, 2018.
- ⁶⁸ C. Z. Hadad, Elizabeth Florez, Gabriel Merino, José Luis Cabellos, Franklin Ferraro, and Albeiro Restrepo. Potential energy surfaces of WC_6 clusters in different spin states. *The Journal of Physical Chemistry A*, 118(31):5762–5768, 2014. PMID: 24533862.
- ⁶⁹ Martin Saunders. Stochastic search for isomers on a quantum mechanical surface. *Journal of Computational Chemistry*, 25(5):621–626, 2004.
- ⁷⁰ Martin Saunders. Stochastic exploration of molecular mechanics energy surfaces. hunting for the global minimum. *Journal of the American Chemical Society*, 109(10):3150–3152, 1987.
- ⁷¹ Rafael Grande-Aztatzi, Paulina R. Martínez-Alanis, José Luis Cabellos, Edison Osorio, Ana Martínez, and Gabriel Merino. Structural evolution of small gold clusters doped by one and two boron atoms. *Journal of Computational Chemistry*, 35(32):2288–2296, 2014.
- ⁷² Jin-Chang Guo, Lin-Yan Feng, Ying-Jin Wang, Said Jalife, Alejandro Vásquez-Espinal, Jose Luis Cabellos, Sudip Pan, Gabriel Merino, and Hua-Jin Zhai. Coaxial triple-layered versus helical $\text{Be}_6\text{B}_{11}^-$ clusters: Dual structural fluxionality and multifold aromaticity. *Angewandte Chemie International Edition*, 56(34):10174–10177, 2017.
- ⁷³ Xue Dong, Said Jalife, Alejandro Vásquez-Espinal, Estefanía Ravell, Sudip Pan, José Luis Cabellos, Wei-yan Liang, Zhong-hua Cui, and Gabriel Merino. Li_2B_{12} and Li_3B_{12} : Prediction of the smallest tubular and Cage-like boron structures. *Angewandte Chemie International Edition*, 57(17):4627–4631, 2018.
- ⁷⁴ Sukanta Mondal, Jose Luis Cabellos, Sudip Pan, Edison Osorio, Juan Jose Torres-Vega, William Tiznado, Albeiro Restrepo, and Gabriel Merino. 10- π -electron arenes a la carte: structure and bonding of the $[\text{E}-(\text{C}_n\text{H}_n)-\text{E}]n-6$ ($\text{E} = \text{Ca, Sr, Ba}; n = 6-8$) complexes. *Phys. Chem. Chem. Phys.*, 18:11909–11918, 2016.
- ⁷⁵ P. L. Rodríguez-Kessler, Sudip Pan, Elizabeth Florez, José Luis Cabellos, and Gabriel Merino. Structural evolution of the rhodium-doped silver clusters Ag_nR_h ($n < 15$) and their reactivity toward no. *The Journal of Physical Chemistry C*, 121(35):19420–19427, 2017.
- ⁷⁶ Anastassia N. Alexandrova, Alexander I. Boldyrev, You-Jun Fu, Xin Yang, Xue-Bin Wang, and Lai-Sheng Wang. Structure of the Na_xCl_x ($x=1,4$) clusters via ab-initio genetic algorithm and photoelectron spectroscopy. *J. Chem. Phys.*, 121(12):5709–5719, 2004.
- ⁷⁷ Nicholas T. Wilson and Roy L. Johnston. A theoretical study of atom ordering in copper–gold nanoalloy clusters. *J. Mater. Chem.*, 12:2913–2922, 2002.
- ⁷⁸ Fabrizio Cleri and Vittorio Rosato. Tight-binding potentials for transition metals and alloys. *Phys. Rev. B*, 48:22–33, Jul 1993.
- ⁷⁹ M. J. Frisch, G. W. Trucks, H. B. Schlegel, G. E. Scuseria, M. A. Robb, J. R. Cheeseman, G. Scalmani, V. Barone, B. Mennucci, G. A. Petersson, H. Nakatsuji, M. Cariati, X. Li, H. P. Hratchian, A. F. Izmaylov, J. Bloino, G. Zheng, J. L. Sonnenberg, M. Hada, M. Ehara, K. Toyota, R. Fukuda, J. Hasegawa, M. Ishida, T. Nakajima, Y. Honda, O. Kitao, H. Nakai, T. Vreven, J. A. Montgomery, J. E. Peralta, F. Ogliaro, M. Bearpark, J. J. Heyd, E. Brothers, K. N. Kudin, V. N. Staroverov, R. Kobayashi, J. Normand, K. Raghavachari, A. Rentzsch, J. C. Burant, S. S. Iyengar, J. Tomasi, M. Cossi, N. Rega, J. M. Millam, M. Klene, J. E. Knox, J. B. Cross, V. Bakken, C. Adamo, J. Jaramillo, R. Gomperts, R. E. Stratmann, O. Yazyev, A. J. Austin, R. Cammi, C. Pomelli, J. W. Ochterski, R. L. Martin, K. Morokuma, V. G. Zakrzewski, G. A. Voth, P. Salvador, J. J. Dannenberg, S. Dapprich, A. D. Daniels, Farkas, J. B. Foresman, J. V. Ortiz, J. Cioslowski, and D. J. Fox. Gaussian 09, 2009.
- ⁸⁰ Stefan Grimme, Jens Antony, Stephan Ehrlich, and Helge Krieg. A consistent and accurate ab initio parametrization of density functional dispersion correction (DFT-D) for the 94 elements H-Pu. *The Journal of Chemical Physics*, 132(15):154104, 2010.
- ⁸¹ Axel D. Becke. Density-functional thermochemistry III. the role of exact exchange. *The Journal of Chemical Physics*, 98(7):5648–5652, 1993.
- ⁸² A. D. Becke. Density-functional exchange-energy approximation with correct asymptotic behavior. *Phys. Rev. A*, 38:3098–3100, Sep 1988.
- ⁸³ John P. Perdew and Yue Wang. Accurate and simple analytic representation of the electron-gas correlation energy. *Phys. Rev. B*, 45:13244–13249, Jun 1992.
- ⁸⁴ John P. Perdew, Kieron Burke, and Matthias Ernzerhof. Generalized gradient approximation made simple. *Phys. Rev. Lett.*, 77:3865–3868, Oct 1996.
- ⁸⁵ Jorge M. del Campo, José L. Gázquez, S. B. Trickey, and Alberto Vela. Non-empirical improvement of PBE and its hybrid PBE0 for general description of molecular properties. *The Journal of Chemical Physics*, 136(10):104108, 2012.

- ⁸⁶ T. H. Jr. Dunning and P. J. Hay. Modern theoretical chemistry vol. 3. In H. F Schaefer-III, editor, *Methods of Electronic Structure Theory*, chapter 1, pages 1–28. Springer US, Plenum, New York, 1977.
- ⁸⁷ F. Sue Legge, Graeme L. Nyberg, and J. Barrie Peel. DFT calculations for Cu-, Ag-, and Au-containing molecules. *The Journal of Physical Chemistry A*, 105(33):7905–7916, 2001.
- ⁸⁸ Florian Weigend and Reinhart Ahlrichs. Balanced basis sets of split valence, triple zeta valence and quadruple zeta valence quality for H to Rn: Design and assessment of accuracy. *Phys. Chem. Chem. Phys.*, 7:3297–3305, 2005.
- ⁸⁹ Shuqiang Niu, Dao-Ling Huang, Phuong D. Dau, Hong-Tao Liu, Lai-Sheng Wang, and Toshiko Ichiye. Assessment of quantum mechanical methods for copper and iron complexes by photoelectron spectroscopy. *Journal of Chemical Theory and Computation*, 10(3):1283–1291, 2014. PMID: 24803858.
- ⁹⁰ Eugenia Dzib, José Luis Cabellos, Filiberto Ortíz-Chi, Sudip Pan, Annia Galano, and Gabriel Merino. Eyringpy: A program for computing rate constants in the gas phase and in solution. *International Journal of Quantum Chemistry*, 119(2):e25686, 2019.
- ⁹¹ Akira Takada, Reinhard Conradt, and Pascal Richet. Partition function and configurational entropy in non-equilibrium states: A new theoretical model. *Entropy*, 20(4), 2018.
- ⁹² Georg Brehm, Markus Reiher, Boris Le Guennic, Michael Leibold, Siegfried Schindler, Frank W. Heinemann, and Siegfried Schneider. Investigation of the low-spin to high-spin transition in a novel [Fe(pmea)(NCS)2] complex by IR and raman spectroscopy and DFT calculations. *Journal of Raman Spectroscopy*, 37(1-3):108–122, 2006.
- ⁹³ Philipp Pracht and Stefan Grimme. Calculation of absolute molecular entropies and heat capacities made simple. *Chem. Sci.*, 12:6551–6568, 2021.
- ⁹⁴ D.A. McQuarrie and M.Q.D. A. *Statistical Mechanics*. Chemistry Series. Harper & Row, 1975.
- ⁹⁵ T.L. Hill. *An Introduction to Statistical Thermodynamics*. Addison-Wesley series in chemistry. Dover Publications, 1986.
- ⁹⁶ Saswata Bhattacharya, Daniel Berger, Karsten Reuter, Luca M. Ghiringhelli, and Sergey V. Levchenko. Theoretical evidence for unexpected O-rich phases at corners of MgO surfaces. *Phys. Rev. Materials*, 1:071601, Dec 2017.
- ⁹⁷ Preeti Bhumla, Manish Kumar, and Saswata Bhattacharya. Theoretical insights into C-H bond activation of methane by transition metal clusters: the role of anharmonic effects. *Nanoscale Adv.*, 3:575–583, 2021.
- ⁹⁸ David Shortle. Propensities, probabilities, and the boltzmann hypothesis. *Computational and Theoretical Chemistry*, 12:1298–1302, 2003.
- ⁹⁹ D. Schebarchov, F. Baletto, and D. J. Wales. Structure, thermodynamics, and rearrangement mechanisms in gold clusters—insights from the energy landscapes framework. *Nanoscale*, 10:2004–2016, 2018.
- ¹⁰⁰ Bryan R. Goldsmith, Jacob Florian, Jin-Xun Liu, Philipp Gruene, Jonathan T. Lyon, David M. Rayner, André Fielicke, Matthias Scheffler, and Luca M. Ghiringhelli. Two-to-three dimensional transition in neutral gold clusters: The crucial role of van der waals interactions and temperature. *Phys. Rev. Materials*, 3:016002, Jan 2019.
- ¹⁰¹ Mukul Kabir, Abhijit Mookerjee, and A. K. Bhattacharya. Structure and stability of copper clusters: A tight-binding molecular dynamics study. *Phys. Rev. A*, 69:043203, Apr 2004.
- ¹⁰² Galip H. Guvelioglu, Pingping Ma, Xiaoyi He, Robert C. Forrey, and Hansong Cheng. First principles studies on the growth of small Cu clusters and the dissociative chemisorption of H₂. *Phys. Rev. B*, 73:155436, Apr 2006.
- ¹⁰³ Jianhua Zhang, Cai-Zhuang Wang, Zizhong Zhu, Qing Huo Liu, and Kai-Ming Ho. Multimode Jahn-Teller effect in bulk systems: A case of the Nv⁰ center in diamond. *Phys. Rev. B*, 97:165204, Apr 2018.
- ¹⁰⁴ Matija Zlatar, Maja Gruden-Pavlović, Carl-Wilhelm Schläpfer, and Claude Daul. Intrinsic distortion path in the analysis of the Jahn–Teller effect. *Journal of Molecular Structure: THEOCHEM*, 954(1):86–93, 2010. DFT09, 13th International Conference on the Applications of Density Functional Theory in Chemistry and Physics.
- ¹⁰⁵ U. Opik and Maurice Henry Lecorney Pryce. Studies of the Jahn-Teller effect. i. a survey of the static problem. *Proceedings of the Royal Society of London. Series A. Mathematical and Physical Sciences*, 238(1215):425–447, 1957.
- ¹⁰⁶ Stan J. Tinnemans, J. Gerbrand Mesu, Kaisa Kervinen, Tom Visser, T. Alexander Nijhuis, Andrew M. Beale, Daphne E. Keller, Ad M.J. van der Eerden, and Bert M. Weckhuysen. Combining operando techniques in one spectroscopic-reaction cell: New opportunities for elucidating the active site and related reaction mechanism in catalysis. *Catalysis Today*, 113(1):3–15, 2006. Recent Advances in In situ and Operando Studies of Catalytic Reactions.
- ¹⁰⁷ M. Brandhorst, S. Cristol, M. Capron, C. Dujardin, H. Vezin, G. Le bourdon, and E. Payen. Catalytic oxidation of methanol on Mo/Al₂O₃ catalyst: An EPR and raman/infrared operando spectroscopies study. *Catalysis Today*, 113(1):34–39, 2006. Recent Advances in In situ and Operando Studies of Catalytic Reactions.
- ¹⁰⁸ Kazuki Hashimoto, Venkata Ramaiah Badarla, Akira Kawai, and Takuro Ideguchi. Complementary vibrational spectroscopy. *Nature Communications*, 10(1):4411, Sep 2019.
- ¹⁰⁹ A. Fielicke, G. von Helden, and G. Meijer. Far-infrared spectroscopy of isolated transition metal clusters. *The European Physical Journal D - Atomic, Molecular, Optical and Plasma Physics*, 34(1):83–88, Jul 2005.
- ¹¹⁰ D. E. Powers, S. G. Hansen, M. E. Geusic, A. C. Puiu, J. B. Hopkins, T. G. Dietz, M. A. Duncan, P. R. R. Langridge-Smith, and R. E. Smalley. Supersonic metal cluster beams: laser photoionization studies of copper cluster (Cu₂). *The Journal of Physical Chemistry*, 86(14):2556–2560, 1982.
- ¹¹¹ Olga V. Lushchikova, Douwe M. M. Huitema, Pablo López-Tarifa, Lucas Visscher, Zahra Jamshidi, and Joost M. Bakker. Structures of Cu_n⁺ (n = 3–10) clusters obtained by infrared action spectroscopy. *The Journal of Physical Chemistry Letters*, 10(9):2151–2155, 2019. PMID: 30977666.
- ¹¹² Takeshi Yanai, David P Tew, and Nicholas C Handy. A new hybrid exchange-correlation functional using the coulomb-attenuating method (CAM-B3LYP). *Chemical Physics Letters*, 393(1):51–57, 2004.
- ¹¹³ S. Lecoutre, A. Rydlo, C. Felix, J. Buttet, S. Gilb, and W. Harbich. Optical absorption of small copper clusters in neon: Cu_n, (n = 1–9). *The Journal of Chemical Physics*, 134(7):074303, 2011.

- ¹¹⁴ Christoph Sieber, Jean Buttet, Wolfgang Harbich, Christian Félix, Roland Mitić, and Vlasta Bonačić Koutecký. Isomer-specific spectroscopy of metal clusters trapped in a matrix: Ag₉. *Phys. Rev. A*, 70:041201, Oct 2004.
- ¹¹⁵ Vivike J. F. Lapoutre, Marko Haertelt, Gerard Meijer, André Fielicke, and Joost M. Bakker. Communication: IR spectroscopy of neutral transition metal clusters through thermionic emission. *The Journal of Chemical Physics*, 139(12):121101, 2013.
- ¹¹⁶ Cesar Castillo-Quevedo, Jose Luis Cabellos, Raul Aceves, Roberto Núñez-González, and Alvaro Posada-Amarillas. Cu-doped KCl unfolded band structure and optical properties studied by DFT calculations. *Materials*, 13(19), 2020.
- ¹¹⁷ Gerald Geudtner, Patrizia Calaminici, Javier Carmona-Espíndola, Jorge Martín del Campo, Víctor Daniel Domínguez-Soria, Robert Flores Moreno, Gabriel Ulises Gamboa, Annick Goursot, Andreas M. Köster, José Ulises Reveles, Tzonka Mineva, José Manuel Vásquez-Pérez, Alberto Vela, Bernardo Zúñiga Gutierrez, and Dennis R. Salahub. deMon2k. *WIREs Computational Molecular Science*, 2(4):548–555, 2012.
- ¹¹⁸ Andreas M. Koster, J. Ulises Reveles, and Jorge M. del Campo. Calculation of exchange-correlation potentials with auxiliary function densities. *The Journal of Chemical Physics*, 121(8):3417–3424, 2004.

Appendix A: ZPE descomposition

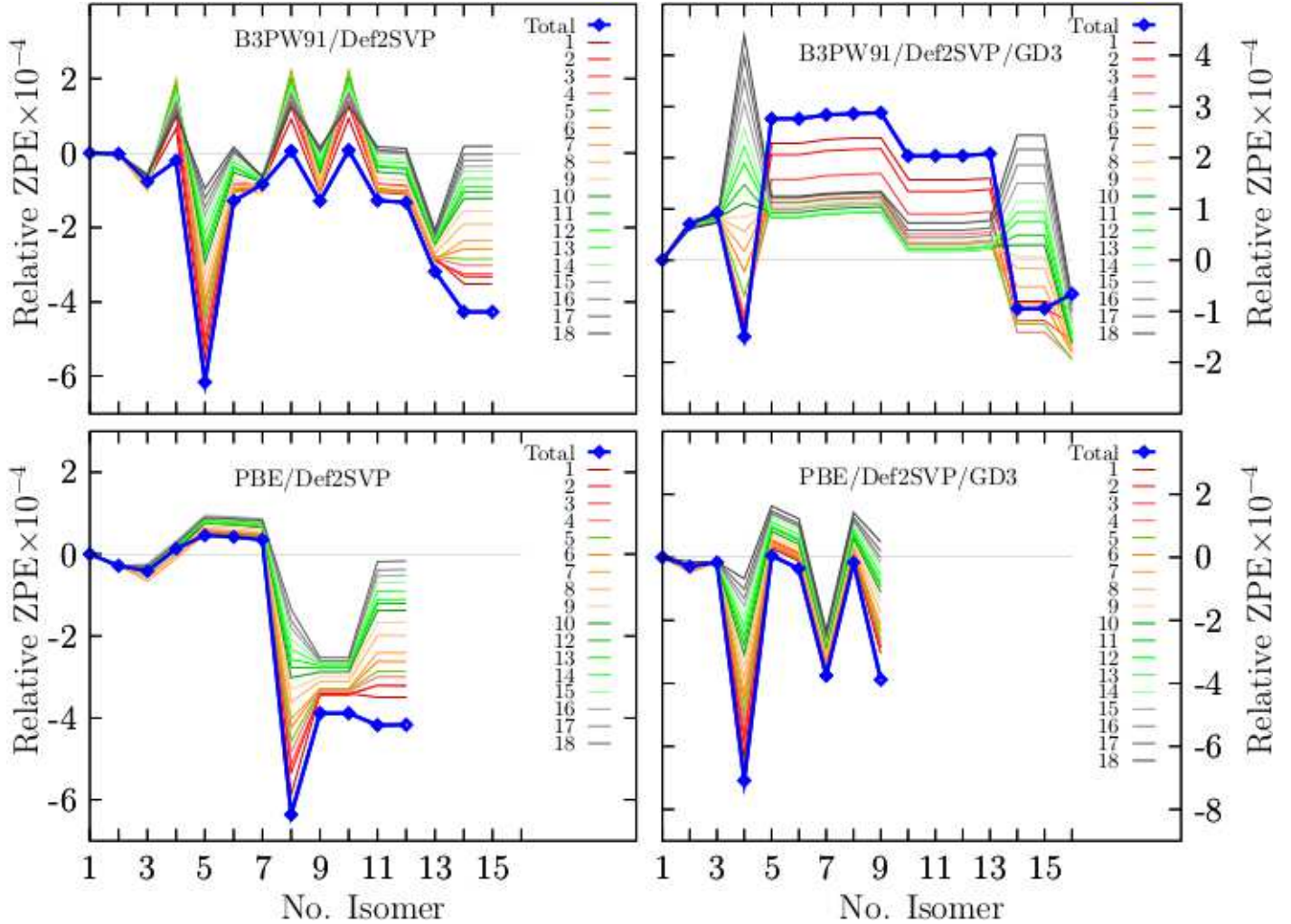


FIG. 5: (Color online) We show the relative zero-point energy (ZPE) decomposition as a function of the vibrational modes (Hartree/particle). In the x-axis are the isomers arranged from the lowest-energy isomer (1) to higher energy isomers (14).

Appendix B: IR spectra

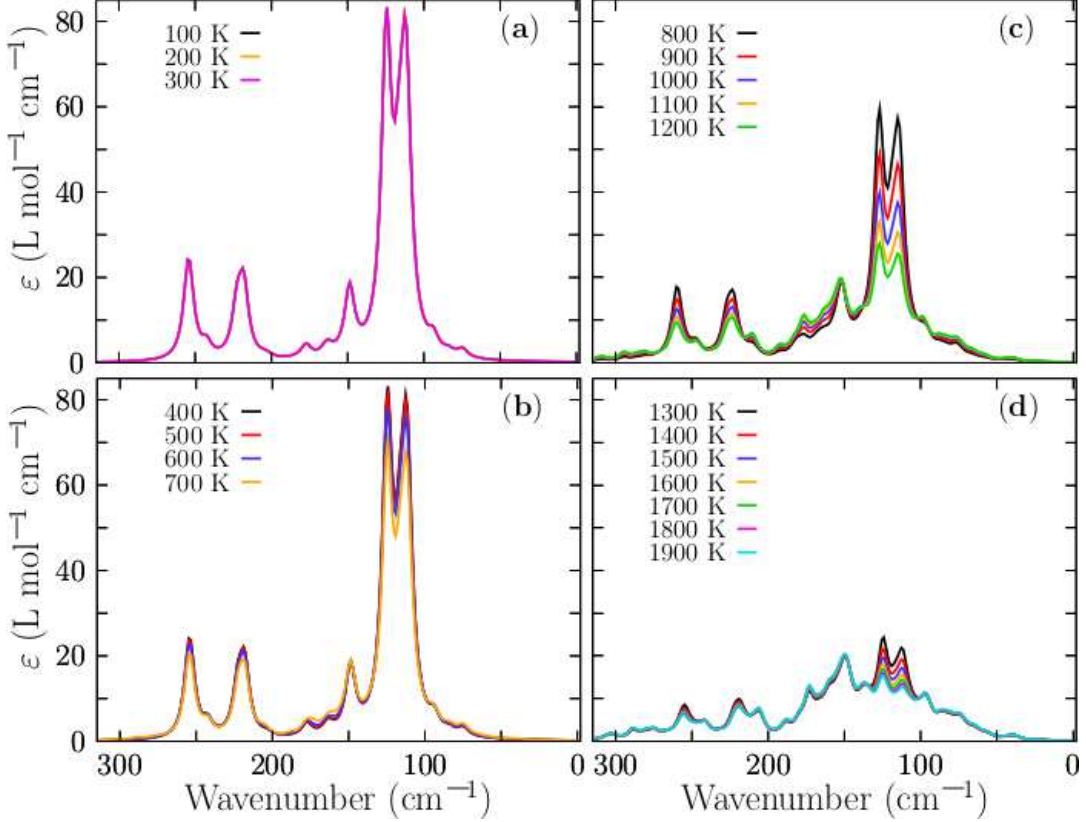


FIG. 6: The dependent temperature IR Boltzmann-spectra-weighted at room temperature of the neutral Cu₃₈ cluster are shown in panels (a) to (d) for different temperatures. The computed IR spectrum of each isomer is multiplied by their corresponding Boltzmann weight at finite temperature; then, they are summed together to produce a final Boltzmann-weighted IR spectrum. Each spectrum of each isomer were computed employing time-dependent density functional theory (TD-DFT) as implemented in Gaussian code at the B3PW91/def2-TZVP level of theory employing geometries optimized at B3PW91-D3/def2-SVP. The large change in the IR spectra occur at temperature of 824 K, as we can see in in the panel (d), and in good agreement with the relative occurrence displayed in Figure 2.

Appendix C: UV-Visible spectra for different temperatures

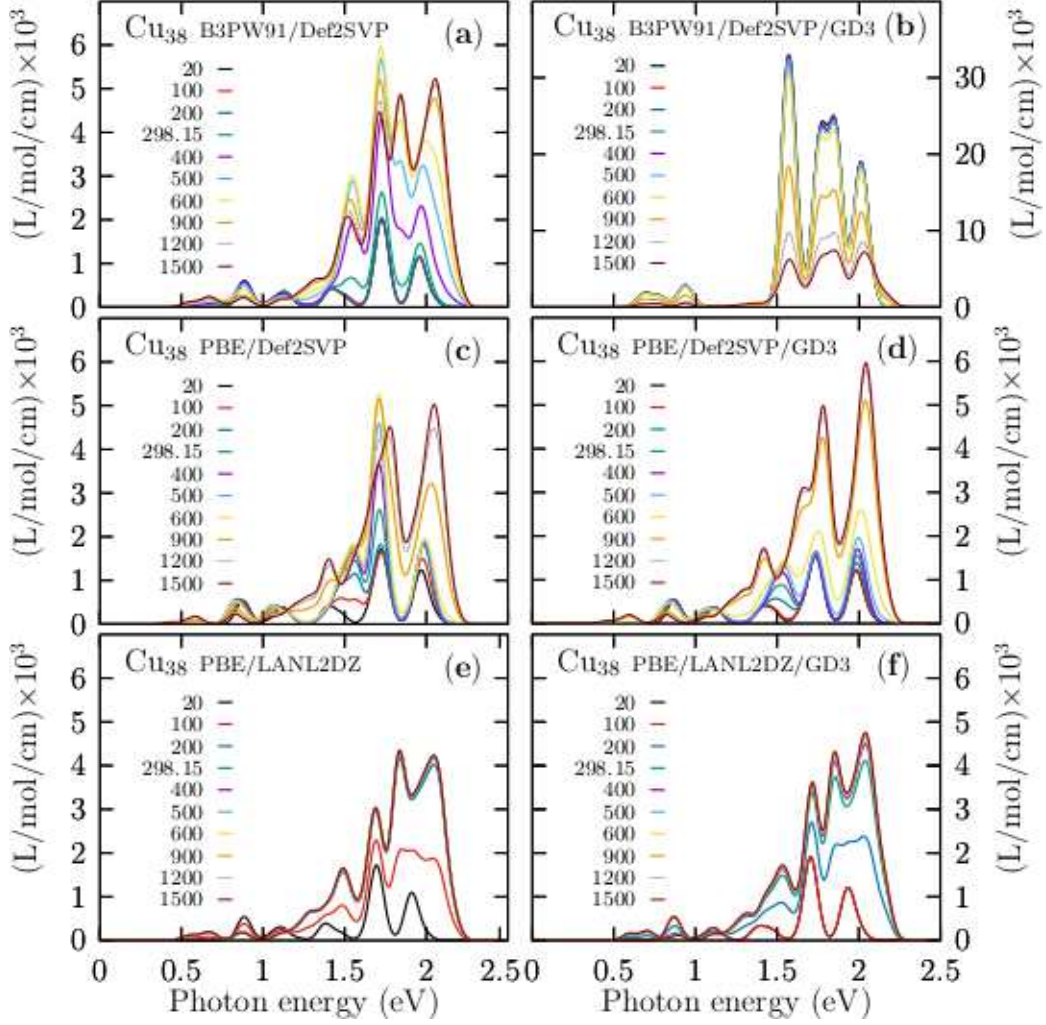


FIG. 7: (Color online) The dependent temperature UV-visible Boltzmann-spectra-weighted at room temperature of the neutral Cu₃₈ cluster are shown in panels (e) to (g) with Grimme's dispersion GD3 (without GD3 panels (a) to (d)) The computed UV-visible spectrum of each isomer is multiplied by their corresponding Boltzmann weight at finite temperature; then, they are summed together to produce a final Boltzmann-weighted IR spectrum. Each spectrum of each isomer were computed employing time-dependent density functional theory (TD-DFT) as implemented in Gaussian code at the CAM B3LYP/def2-SVP level of theory employing geometries optimized at B3PW91-D3/def2-SVP.

Appendix D: Geometry at B3PW91/Def2svp level of theory

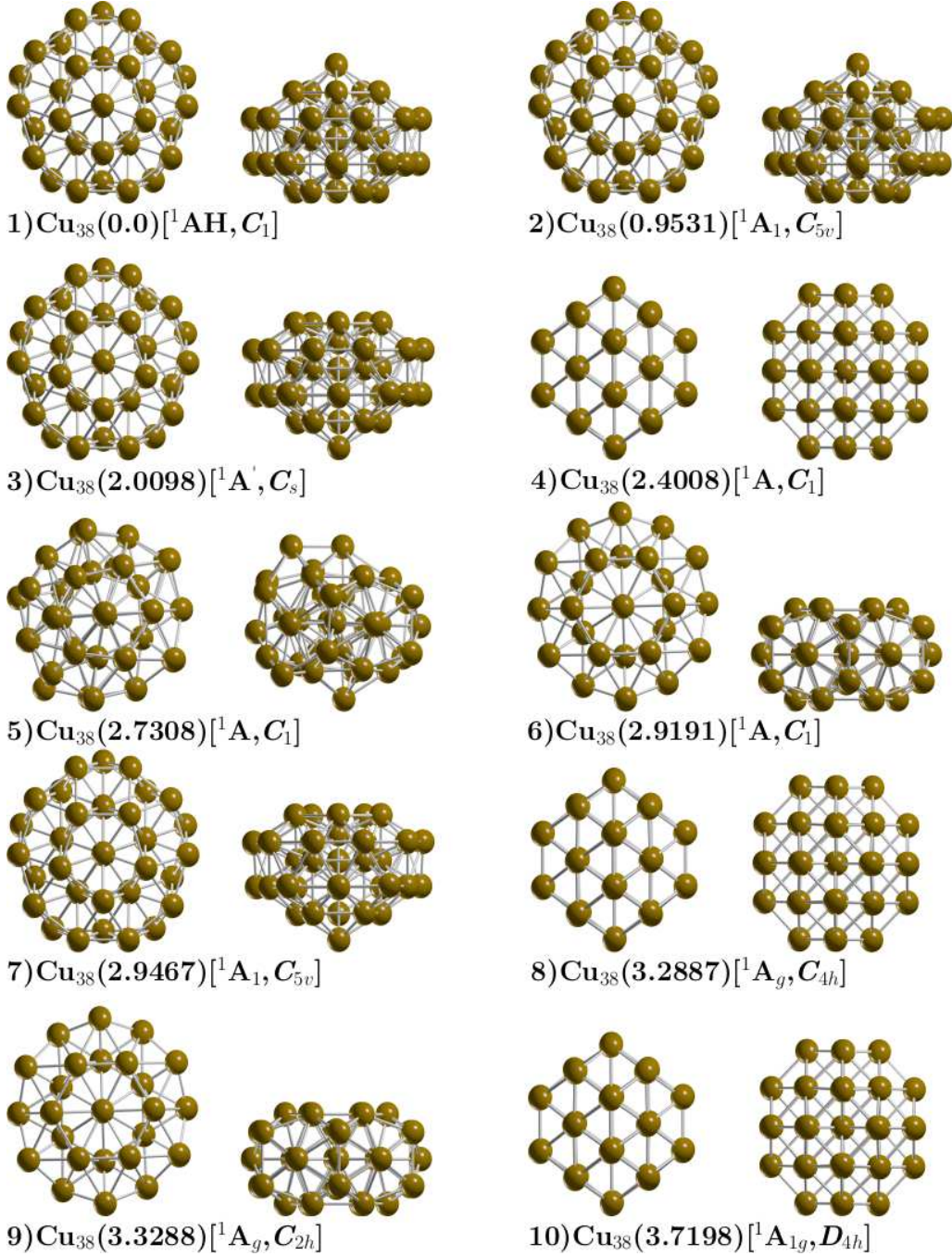


FIG. 8: (Color online) Optimized geometries in front and side views of neutral Cu_{38} cluster at B3PW91/def2-SVP level of theory. The first letter is the isomer label, relative Gibbs free energies in kcal/mol (in round parenthesis) at 298.15 K, electronic group and group symmetry point [in square parenthesis], the probability of occurrence (in red round parenthesis) at 298.15 K.

Appendix E: XYZ atomic coordiantes

38

0.000000000 gibss_0001.out

Cu	-1.741167000000	-0.158313000000	3.424442000000
Cu	-1.777542000000	-0.161558000000	-0.000026000000
Cu	-0.158340000000	1.741115000000	3.424465000000
Cu	0.158346000000	-1.741130000000	-3.424473000000
Cu	-1.638340000000	-1.965976000000	-1.760408000000
Cu	-1.965973000000	1.638364000000	-1.760399000000
Cu	-0.161559000000	1.777542000000	0.000001000000
Cu	1.741184000000	0.158312000000	-3.424443000000
Cu	-1.638381000000	-1.965997000000	1.760353000000
Cu	1.965966000000	-1.638365000000	1.760395000000
Cu	-0.000022000000	-0.000001000000	1.661034000000
Cu	0.158252000000	-1.741146000000	3.424462000000
Cu	2.092781000000	-3.341499000000	0.000013000000
Cu	3.341505000000	2.092789000000	0.000059000000
Cu	1.777542000000	0.161558000000	0.000020000000
Cu	0.317743000000	-3.496543000000	1.724356000000
Cu	0.317778000000	-3.496524000000	-1.724370000000
Cu	-3.496557000000	-0.317767000000	1.724319000000
Cu	3.496520000000	0.317741000000	1.724395000000
Cu	-1.966017000000	1.638350000000	1.760362000000
Cu	3.664053000000	-1.455978000000	0.000035000000
Cu	0.161557000000	-1.777536000000	-0.000006000000
Cu	-3.341499000000	-2.092782000000	-0.000042000000
Cu	-3.664057000000	1.455992000000	-0.000039000000
Cu	3.496552000000	0.317775000000	-1.724315000000
Cu	1.638379000000	1.966002000000	-1.760352000000
Cu	1.741096000000	0.158279000000	3.424485000000
Cu	-0.317788000000	3.496524000000	1.724365000000
Cu	-1.741081000000	-0.158288000000	-3.424488000000
Cu	1.966013000000	-1.638353000000	-1.760365000000
Cu	-0.158253000000	1.741137000000	-3.424459000000
Cu	-0.317738000000	3.496539000000	-1.724349000000
Cu	-1.455990000000	-3.664048000000	-0.000025000000
Cu	0.000024000000	0.000009000000	-1.661040000000
Cu	-2.092798000000	3.341499000000	-0.000013000000
Cu	1.455986000000	3.664055000000	0.000042000000
Cu	-3.496517000000	-0.317760000000	-1.724399000000
Cu	1.638342000000	1.965984000000	1.760408000000

38

0.169425003 mol_0002.out

Cu	3.513500000000	1.796474000000	0.000001000000
Cu	0.001079000000	1.772700000000	-0.000004000000
Cu	3.516966000000	-0.002124000000	-1.698724000000
Cu	-3.516961000000	0.002132000000	1.698727000000
Cu	-1.808652000000	1.810631000000	1.758032000000
Cu	-1.808655000000	1.810629000000	-1.758028000000
Cu	0.000024000000	-0.000012000000	-1.680316000000
Cu	-3.513525000000	-1.796471000000	-0.000010000000
Cu	1.810831000000	1.808461000000	1.758030000000
Cu	1.808648000000	-1.810647000000	1.758046000000
Cu	1.771217000000	-0.001082000000	0.000009000000
Cu	3.516981000000	-0.002120000000	1.698709000000
Cu	-0.001045000000	-1.735089000000	3.435940000000
Cu	-0.002123000000	-3.498863000000	-1.735691000000

Cu -0.001088000000 -1.772720000000 0.000003000000
Cu 1.769137000000 -0.001066000000 3.418064000000
Cu -1.769051000000 0.001079000000 3.418037000000
Cu 1.765981000000 3.525659000000 -0.000002000000
Cu 1.761732000000 -3.527775000000 0.000020000000
Cu 1.810839000000 1.808464000000 -1.758034000000
Cu -0.002148000000 -3.498870000000 1.735669000000
Cu 0.000016000000 -0.000009000000 1.680314000000
Cu 0.002097000000 3.498861000000 1.735676000000
Cu 0.002097000000 3.498863000000 -1.735698000000
Cu -1.766014000000 -3.525655000000 -0.000018000000
Cu -1.810842000000 -1.808450000000 -1.758047000000
Cu 3.511350000000 -1.800707000000 0.000022000000
Cu 1.769120000000 -0.001061000000 -3.418053000000
Cu -3.511372000000 1.800704000000 0.000010000000
Cu -1.810841000000 -1.808447000000 1.758028000000
Cu -3.516989000000 0.002137000000 -1.698717000000
Cu -1.769072000000 0.001075000000 -3.418030000000
Cu 0.001057000000 1.735091000000 3.435939000000
Cu -1.771212000000 0.001074000000 -0.000010000000
Cu 0.001046000000 1.735085000000 -3.435936000000
Cu -0.001046000000 -1.735083000000 -3.435939000000
Cu -1.761741000000 3.527776000000 0.000002000000
Cu 1.808658000000 -1.810644000000 -1.758021000000

38

1.384892499 mol_0003.out

Cu -3.517960000000 1.780496000000 0.000000000000
Cu 0.000000000000 1.785134000000 0.000000000000
Cu -3.510601000000 0.000000000000 1.725845000000
Cu 3.510601000000 0.000000000000 -1.725845000000
Cu 1.809494000000 1.809494000000 -1.759436000000
Cu 1.809494000000 1.809494000000 1.759436000000
Cu 0.000000000000 0.000000000000 1.661000000000
Cu 3.517960000000 -1.780496000000 0.000000000000
Cu -1.809494000000 1.809494000000 -1.759436000000
Cu -1.809494000000 -1.809494000000 -1.759436000000
Cu -1.785134000000 0.000000000000 0.000000000000
Cu -3.510601000000 0.000000000000 -1.725845000000
Cu 0.000000000000 -1.748410000000 -3.423917000000
Cu 0.000000000000 -3.510601000000 1.725845000000
Cu 0.000000000000 -1.785134000000 0.000000000000
Cu -1.748410000000 0.000000000000 -3.423917000000
Cu 1.748410000000 0.000000000000 -3.423917000000
Cu -1.780496000000 3.517960000000 0.000000000000
Cu -1.780496000000 -3.517960000000 0.000000000000
Cu -1.809494000000 1.809494000000 1.759436000000
Cu 0.000000000000 -3.510601000000 -1.725845000000
Cu 0.000000000000 0.000000000000 -1.661000000000
Cu 0.000000000000 3.510601000000 -1.725845000000
Cu 0.000000000000 3.510601000000 1.725845000000
Cu 1.780496000000 -3.517960000000 0.000000000000
Cu 1.809494000000 -1.809494000000 1.759436000000
Cu -3.517960000000 -1.780496000000 0.000000000000
Cu -1.748410000000 0.000000000000 3.423917000000
Cu 3.517960000000 1.780496000000 0.000000000000
Cu 1.809494000000 -1.809494000000 -1.759436000000
Cu 3.510601000000 0.000000000000 1.725845000000
Cu 1.748410000000 0.000000000000 3.423917000000

Cu	0.000000000000	1.748410000000	-3.423917000000
Cu	1.785134000000	0.000000000000	0.000000000000
Cu	0.000000000000	1.748410000000	3.423917000000
Cu	0.000000000000	-1.748410000000	3.423917000000
Cu	1.780496000000	3.517960000000	0.000000000000
Cu	-1.809494000000	-1.809494000000	1.759436000000

38

5.798100000 mol_0006.out			
Cu	1.172939000000	1.097826000000	3.378465000000
Cu	-0.032807000000	-2.145198000000	0.000000000000
Cu	2.431734000000	-0.653745000000	2.012704000000
Cu	-0.938438000000	-2.463862000000	-3.334080000000
Cu	-1.123725000000	-0.000130000000	0.000000000000
Cu	1.173103000000	-2.873666000000	-2.087959000000
Cu	1.172939000000	1.097826000000	-3.378465000000
Cu	-0.938631000000	2.409535000000	-3.373250000000
Cu	-0.032655000000	-0.662804000000	2.040109000000
Cu	-0.032401000000	1.735377000000	1.260561000000
Cu	2.431564000000	1.712147000000	1.243736000000
Cu	-0.938609000000	0.033485000000	4.145587000000
Cu	-2.182325000000	0.675722000000	2.079899000000
Cu	-0.938756000000	3.952969000000	1.249204000000
Cu	-0.938756000000	3.952969000000	-1.249204000000
Cu	1.145976000000	-1.308226000000	4.026584000000
Cu	-2.182373000000	-1.769544000000	1.285501000000
Cu	1.146150000000	-4.233754000000	0.000000000000
Cu	1.145845000000	3.425285000000	2.488512000000
Cu	1.173103000000	-2.873666000000	2.087959000000
Cu	-2.182362000000	2.186891000000	0.000000000000
Cu	-3.439847000000	-0.000200000000	0.000000000000
Cu	-0.938319000000	-3.932561000000	1.312904000000
Cu	2.431736000000	-2.116158000000	0.000000000000
Cu	1.145845000000	3.425285000000	-2.488512000000
Cu	-0.032401000000	1.735377000000	-1.260561000000
Cu	-0.938631000000	2.409535000000	3.373250000000
Cu	1.270655000000	-0.000203000000	0.000000000000
Cu	1.145976000000	-1.308226000000	-4.026584000000
Cu	-2.182373000000	-1.769544000000	-1.285501000000
Cu	-0.938609000000	0.033485000000	-4.145587000000
Cu	-0.032655000000	-0.662804000000	-2.040109000000
Cu	-0.938438000000	-2.463862000000	3.334080000000
Cu	-2.182325000000	0.675722000000	-2.079899000000
Cu	2.431734000000	-0.653745000000	-2.012704000000
Cu	1.172889000000	3.552872000000	0.000000000000
Cu	-0.938319000000	-3.932561000000	-1.312904000000
Cu	2.431564000000	1.712147000000	-1.243736000000

38

5.798100000 mol_0005.out			
Cu	1.105608000000	3.375910000000	-1.172987000000
Cu	-2.145190000000	0.004974000000	0.032902000000
Cu	-0.649183000000	2.014217000000	-2.431704000000
Cu	-2.471547000000	-3.328357000000	0.938545000000
Cu	-0.000079000000	-0.000001000000	1.123724000000
Cu	-2.878554000000	-2.081286000000	-1.172976000000
Cu	1.089932000000	-3.381006000000	-1.172979000000
Cu	2.401746000000	-3.378831000000	0.938519000000
Cu	-0.658068000000	2.041641000000	0.032685000000
Cu	1.738298000000	1.256532000000	0.032323000000

Cu	1.714919000000	1.239763000000	-2.431641000000
Cu	0.043144000000	4.145497000000	0.938610000000
Cu	0.680643000000	2.078324000000	2.182295000000
Cu	3.955899000000	1.240030000000	0.938578000000
Cu	3.950099000000	-1.258371000000	0.938578000000
Cu	-1.298933000000	4.029609000000	-1.145915000000
Cu	-1.766459000000	1.289600000000	2.182453000000
Cu	-4.233794000000	0.009824000000	-1.145961000000
Cu	3.430997000000	2.480561000000	-1.145998000000
Cu	-2.868866000000	2.094620000000	-1.172981000000
Cu	2.186984000000	-0.005073000000	2.182263000000
Cu	-0.000045000000	0.000000000000	3.439846000000
Cu	-3.929462000000	1.322022000000	0.938496000000
Cu	-2.116261000000	0.004912000000	-2.431642000000
Cu	3.419450000000	-2.496451000000	-1.145994000000
Cu	1.732447000000	-1.264583000000	0.032321000000
Cu	2.417399000000	3.367646000000	0.938517000000
Cu	-0.000260000000	0.000001000000	-1.270656000000
Cu	-1.317613000000	-4.023537000000	-1.145918000000
Cu	-1.772420000000	-1.281396000000	2.182451000000
Cu	0.023909000000	-4.145655000000	0.938616000000
Cu	-0.667531000000	-2.038564000000	0.032684000000
Cu	-2.456078000000	3.339789000000	0.938548000000
Cu	0.670994000000	-2.081457000000	2.182292000000
Cu	-0.658520000000	-2.011176000000	-2.431704000000
Cu	3.552810000000	-0.008241000000	-1.173050000000
Cu	-3.935562000000	-1.303783000000	0.938496000000
Cu	1.709147000000	-1.247704000000	-2.431634000000

38

5.810022499 mol_0007.out			
Cu	1.766398000000	-3.082086000000	-1.172799000000
Cu	1.440661000000	1.589530000000	0.032911000000
Cu	1.930492000000	-0.866814000000	-2.431711000000
Cu	-0.816402000000	4.064729000000	0.938172000000
Cu	-0.000031000000	0.000142000000	1.123925000000
Cu	0.382489000000	3.531342000000	-1.172949000000
Cu	-3.240376000000	1.454978000000	-1.172933000000
Cu	-4.118083000000	0.479809000000	0.938149000000
Cu	1.956875000000	-0.878715000000	0.032801000000
Cu	-0.231030000000	-2.132524000000	0.032845000000
Cu	-0.227732000000	-2.103731000000	-2.431572000000
Cu	3.049608000000	-2.808643000000	0.938449000000
Cu	1.087887000000	-1.897327000000	2.182398000000
Cu	-1.728917000000	-3.768022000000	0.938368000000
Cu	-3.580249000000	-2.090260000000	0.938549000000
Cu	3.862306000000	-1.734288000000	-1.146249000000
Cu	2.140799000000	0.448442000000	2.182400000000
Cu	2.842814000000	3.137229000000	-1.146425000000
Cu	-0.455870000000	-4.208980000000	-1.146341000000
Cu	3.477118000000	0.727378000000	-1.172831000000
Cu	-1.468555000000	-1.620845000000	2.182378000000
Cu	-0.000120000000	0.000172000000	3.440164000000
Cu	3.613691000000	2.032444000000	0.938308000000
Cu	1.420985000000	1.567972000000	-2.431672000000
Cu	-4.143913000000	-0.867104000000	-1.146419000000
Cu	-2.099748000000	-0.439303000000	0.032870000000
Cu	0.881639000000	-4.050719000000	0.938679000000
Cu	-0.000046000000	-0.000099000000	-1.269991000000

Cu -2.105204000000 3.672841000000 -1.146580000000
Cu 0.235173000000 2.174649000000 2.182401000000
Cu -3.094383000000 2.758837000000 0.938321000000
Cu -1.066643000000 1.861156000000 0.032997000000
Cu 4.125010000000 -0.413264000000 0.938640000000
Cu -1.995549000000 0.895815000000 2.182347000000
Cu -1.052144000000 1.835710000000 -2.431642000000
Cu -2.385389000000 -2.632250000000 -1.172838000000
Cu 1.667604000000 3.795290000000 0.938410000000
Cu -2.071166000000 -0.433489000000 -2.431532000000
38
6.768842500 mol_0008.out
Cu 3.378495000000 -1.097740000000 -1.172970000000
Cu 0.000000000000 2.145197000000 0.032772000000
Cu 2.012643000000 0.653947000000 -2.431766000000
Cu -3.334103000000 2.463807000000 0.938557000000
Cu 0.000000000000 0.000000000000 1.123689000000
Cu -2.088025000000 2.873919000000 -1.172970000000
Cu -3.378495000000 -1.097740000000 -1.172970000000
Cu -3.373514000000 -2.409562000000 0.938557000000
Cu 2.040204000000 0.662902000000 0.032772000000
Cu 1.260915000000 -1.735501000000 0.032772000000
Cu 1.243882000000 -1.712056000000 -2.431766000000
Cu 4.145535000000 -0.033525000000 0.938557000000
Cu 2.079873000000 -0.675792000000 2.182292000000
Cu 1.249157000000 -3.952998000000 0.938557000000
Cu -1.249157000000 -3.952998000000 0.938557000000
Cu 4.026559000000 1.308308000000 -1.146004000000
Cu 1.285432000000 1.769246000000 2.182292000000
Cu 0.000000000000 4.233775000000 -1.146004000000
Cu 2.488551000000 -3.425196000000 -1.146004000000
Cu 2.088025000000 2.873919000000 -1.172970000000
Cu 0.000000000000 -2.186908000000 2.182292000000
Cu 0.000000000000 0.000000000000 3.439811000000
Cu 1.312925000000 3.932278000000 0.938557000000
Cu 0.000000000000 2.116218000000 -2.431766000000
Cu -2.488551000000 -3.425196000000 -1.146004000000
Cu -1.260915000000 -1.735501000000 0.032772000000
Cu 3.373514000000 -2.409562000000 0.938557000000
Cu 0.000000000000 0.000000000000 -1.270691000000
Cu -4.026559000000 1.308308000000 -1.146004000000
Cu -1.285432000000 1.769246000000 2.182292000000
Cu -4.145535000000 -0.033525000000 0.938557000000
Cu -2.040204000000 0.662902000000 0.032772000000
Cu 3.334103000000 2.463807000000 0.938557000000
Cu -2.079873000000 -0.675792000000 2.182292000000
Cu -2.012643000000 0.653947000000 -2.431766000000
Cu 0.000000000000 -3.552360000000 -1.172970000000
Cu -1.312925000000 3.932278000000 0.938557000000
Cu -1.243882000000 -1.712056000000 -2.431766000000
38
6.771352500 mol_0009.out
Cu 3.378495000000 -1.097740000000 -1.172928000000
Cu 0.000000000000 2.145197000000 0.032814000000
Cu 2.012643000000 0.653947000000 -2.431724000000
Cu -3.334082000000 2.463861000000 0.938439000000
Cu 0.000000000000 0.000000000000 1.123731000000
Cu -2.088025000000 2.873919000000 -1.172928000000

Cu -3.378495000000 -1.097740000000 -1.172928000000
Cu -3.373559000000 -2.409526000000 0.938439000000
Cu 2.040204000000 0.662902000000 0.032814000000
Cu 1.260915000000 -1.735501000000 0.032814000000
Cu 1.243882000000 -1.712056000000 -2.431724000000
Cu 4.145550000000 -0.033581000000 0.938439000000
Cu 2.079873000000 -0.675792000000 2.182334000000
Cu 1.249108000000 -3.953030000000 0.938439000000
Cu -1.249108000000 -3.953030000000 0.938439000000
Cu 4.026559000000 1.308308000000 -1.145962000000
Cu 1.285432000000 1.769246000000 2.182334000000
Cu 0.000000000000 4.233775000000 -1.145962000000
Cu 2.488551000000 -3.425196000000 -1.145962000000
Cu 2.088025000000 2.873919000000 -1.172928000000
Cu 0.000000000000 -2.186908000000 2.182334000000
Cu 0.000000000000 0.000000000000 3.439853000000
Cu 1.312983000000 3.932276000000 0.938439000000
Cu 0.000000000000 2.116218000000 -2.431724000000
Cu -2.488551000000 -3.425196000000 -1.145962000000
Cu -1.260915000000 -1.735501000000 0.032814000000
Cu 3.373559000000 -2.409526000000 0.938439000000
Cu 0.000000000000 0.000000000000 -1.270649000000
Cu -4.026559000000 1.308308000000 -1.145962000000
Cu -1.285432000000 1.769246000000 2.182334000000
Cu -4.145550000000 -0.033581000000 0.938439000000
Cu -2.040204000000 0.662902000000 0.032814000000
Cu 3.334082000000 2.463861000000 0.938439000000
Cu -2.079873000000 -0.675792000000 2.182334000000
Cu -2.012643000000 0.653947000000 -2.431724000000
Cu 0.000000000000 -3.552360000000 -1.172928000000
Cu -1.312983000000 3.932276000000 0.938439000000
Cu -1.243882000000 -1.712056000000 -2.431724000000

38

8.858417499 mol_0012.out

Cu -2.222929000000 -0.666563000000 2.051042000000
Cu 1.100741000000 0.048218000000 -4.162907000000
Cu 1.100741000000 0.048218000000 4.162907000000
Cu 0.236184000000 -2.141805000000 0.000000000000
Cu 0.236315000000 1.732655000000 1.258584000000
Cu -0.955762000000 -1.309398000000 -4.030462000000
Cu 1.100862000000 3.974155000000 1.240609000000
Cu 1.100619000000 -3.944546000000 1.332148000000
Cu 2.353877000000 -1.770962000000 1.286346000000
Cu 2.354134000000 2.188481000000 0.000000000000
Cu -2.222929000000 -0.666563000000 -2.051042000000
Cu 2.353995000000 0.676142000000 -2.081502000000
Cu 2.353995000000 0.676142000000 2.081502000000
Cu 2.353877000000 -1.770962000000 -1.286346000000
Cu -1.009819000000 1.103123000000 3.394227000000
Cu -1.009794000000 3.569354000000 0.000000000000
Cu 0.236445000000 -0.661760000000 -2.036789000000
Cu -2.223003000000 1.744823000000 1.267637000000
Cu -2.223003000000 1.744823000000 -1.267637000000
Cu -0.955915000000 -4.237971000000 0.000000000000
Cu 1.100862000000 3.974155000000 -1.240609000000
Cu -0.955746000000 3.428780000000 2.490848000000
Cu -0.955762000000 -1.309398000000 4.030462000000
Cu -3.425186000000 0.000016000000 0.000000000000

Cu -0.955746000000 3.428780000000 -2.490848000000
Cu -1.019001000000 -0.000005000000 0.000000000000
Cu 1.100619000000 -3.944546000000 -1.332148000000
Cu -1.009814000000 -2.887484000000 2.098006000000
Cu -1.009819000000 1.103123000000 -3.394227000000
Cu 1.100737000000 2.408075000000 3.395964000000
Cu 1.100737000000 2.408075000000 -3.395964000000
Cu 1.100752000000 -2.485827000000 3.339602000000
Cu -1.009814000000 -2.887484000000 -2.098006000000
Cu 1.100752000000 -2.485827000000 -3.339602000000
Cu 0.236445000000 -0.661760000000 2.036789000000
Cu 0.236315000000 1.732655000000 -1.258584000000
Cu -2.223136000000 -2.156773000000 0.000000000000
Cu 1.428174000000 -0.000159000000 0.000000000000

38

8.858417499 mol_0010.out
Cu -2.222929000000 -0.666563000000 2.051042000000
Cu 1.100741000000 0.048218000000 -4.162907000000
Cu 1.100741000000 0.048218000000 4.162907000000
Cu 0.236184000000 -2.141805000000 0.000000000000
Cu 0.236315000000 1.732655000000 1.258584000000
Cu -0.955762000000 -1.309398000000 -4.030462000000
Cu 1.100862000000 3.974155000000 1.240609000000
Cu 1.100619000000 -3.944546000000 1.332148000000
Cu 2.353877000000 -1.770962000000 1.286346000000
Cu 2.354134000000 2.188481000000 0.000000000000
Cu -2.222929000000 -0.666563000000 -2.051042000000
Cu 2.353995000000 0.676142000000 -2.081502000000
Cu 2.353995000000 0.676142000000 2.081502000000
Cu 2.353877000000 -1.770962000000 -1.286346000000
Cu -1.009819000000 1.103123000000 3.394227000000
Cu -1.009794000000 3.569354000000 0.000000000000
Cu 0.236445000000 -0.661760000000 -2.036789000000
Cu -2.223003000000 1.744823000000 1.267637000000
Cu -2.223003000000 1.744823000000 -1.267637000000
Cu -0.955915000000 -4.237971000000 0.000000000000
Cu 1.100862000000 3.974155000000 -1.240609000000
Cu -0.955746000000 3.428780000000 2.490848000000
Cu -0.955762000000 -1.309398000000 4.030462000000
Cu -3.425186000000 0.000016000000 0.000000000000
Cu -0.955746000000 3.428780000000 -2.490848000000
Cu -1.019001000000 -0.000005000000 0.000000000000
Cu 1.100619000000 -3.944546000000 -1.332148000000
Cu -1.009814000000 -2.887484000000 2.098006000000
Cu -1.009819000000 1.103123000000 -3.394227000000
Cu 1.100737000000 2.408075000000 3.395964000000
Cu 1.100737000000 2.408075000000 -3.395964000000
Cu 1.100752000000 -2.485827000000 3.339602000000
Cu -1.009814000000 -2.887484000000 -2.098006000000
Cu 1.100752000000 -2.485827000000 -3.339602000000
Cu 0.236445000000 -0.661760000000 2.036789000000
Cu 0.236315000000 1.732655000000 -1.258584000000
Cu -2.223136000000 -2.156773000000 0.000000000000
Cu 1.428174000000 -0.000159000000 0.000000000000

38

8.858417499 mol_0011.out
Cu 0.672221000000 -2.049247000000 2.223083000000
Cu -0.059920000000 4.162819000000 -1.100824000000

Cu -0.036451000000 -4.163096000000 -1.100801000000
 Cu 2.141760000000 0.006043000000 -0.236583000000
 Cu -1.729069000000 -1.263491000000 -0.236235000000
 Cu 1.298094000000 4.034150000000 0.955790000000
 Cu -3.970563000000 -1.251894000000 -1.100768000000
 Cu 3.948301000000 -1.320963000000 -1.100682000000
 Cu 1.774377000000 -1.281426000000 -2.354043000000
 Cu -2.188620000000 -0.006173000000 -2.354039000000
 Cu 0.660641000000 2.053007000000 2.223109000000
 Cu -0.682173000000 2.079574000000 -2.354024000000
 Cu -0.670447000000 -2.083396000000 -2.354016000000
 Cu 1.767129000000 1.291436000000 -2.354026000000
 Cu -1.093350000000 -3.397286000000 1.009804000000
 Cu -3.569419000000 -0.010064000000 1.009902000000
 Cu 0.656027000000 2.038749000000 -0.236504000000
 Cu -1.741143000000 -1.272370000000 2.223069000000
 Cu -1.748290000000 1.262528000000 2.223051000000
 Cu 4.237851000000 0.011942000000 0.955925000000
 Cu -3.977546000000 1.229473000000 -1.100771000000
 Cu -3.421480000000 -2.500517000000 0.955912000000
 Cu 1.320844000000 -4.026777000000 0.955790000000
 Cu 0.000128000000 -0.000004000000 3.425264000000
 Cu -3.435520000000 2.481187000000 0.955890000000
 Cu 0.000233000000 0.000006000000 1.018926000000
 Cu 3.940814000000 1.343224000000 -1.100653000000
 Cu 2.893107000000 -2.089651000000 1.009758000000
 Cu -1.112498000000 3.391098000000 1.009796000000
 Cu -2.398514000000 -3.402684000000 -1.100749000000
 Cu -2.417655000000 3.389102000000 -1.100768000000
 Cu 2.495270000000 -3.332592000000 -1.100784000000
 Cu 2.881258000000 2.105925000000 1.009769000000
 Cu 2.476438000000 3.346598000000 -1.100752000000
 Cu 0.667537000000 -2.035027000000 -0.236513000000
 Cu -1.736160000000 1.253722000000 -0.236234000000
 Cu 2.156758000000 0.006076000000 2.223139000000
 Cu 0.000029000000 -0.000002000000 -1.428204000000

38

9.817865000 mol_0013.out

Cu 2.051086000000 0.666438000000 2.222906000000
 Cu -4.162907000000 -0.048223000000 -1.100760000000
 Cu 4.162907000000 -0.048223000000 -1.100760000000
 Cu 0.000000000000 2.141804000000 -0.236213000000
 Cu 1.258921000000 -1.732756000000 -0.236213000000
 Cu -4.030411000000 1.309560000000 0.955736000000
 Cu 1.240546000000 -3.974062000000 -1.100760000000
 Cu 1.332272000000 3.944258000000 -1.100760000000
 Cu 1.286559000000 1.770796000000 -2.353905000000
 Cu 0.000000000000 -2.188825000000 -2.353905000000
 Cu -2.051086000000 0.666438000000 2.222906000000
 Cu -2.081696000000 -0.676384000000 -2.353905000000
 Cu 2.081696000000 -0.676384000000 -2.353905000000
 Cu -1.286559000000 1.770796000000 -2.353905000000
 Cu 3.394305000000 -1.102877000000 1.009805000000
 Cu 0.000000000000 -3.568984000000 1.009805000000
 Cu -2.036977000000 0.661854000000 -0.236213000000
 Cu 1.267641000000 -1.744758000000 2.222906000000
 Cu -1.267641000000 -1.744758000000 2.222906000000
 Cu 0.000000000000 4.237825000000 0.955736000000

Cu -1.240546000000 -3.974062000000 -1.100760000000
 Cu 2.490931000000 -3.428472000000 0.955736000000
 Cu 4.030411000000 1.309560000000 0.955736000000
 Cu 0.000000000000 0.000000000000 3.425167000000
 Cu -2.490931000000 -3.428472000000 0.955736000000
 Cu 0.000000000000 0.000000000000 1.018982000000
 Cu -1.332272000000 3.944258000000 -1.100760000000
 Cu 2.097796000000 2.887369000000 1.009805000000
 Cu -3.394305000000 -1.102877000000 1.009805000000
 Cu 3.396207000000 -2.407882000000 -1.100760000000
 Cu -3.396207000000 -2.407882000000 -1.100760000000
 Cu 3.339518000000 2.485909000000 -1.100760000000
 Cu -2.097796000000 2.887369000000 1.009805000000
 Cu -3.339518000000 2.485909000000 -1.100760000000
 Cu 2.036977000000 0.661854000000 -0.236213000000
 Cu -1.258921000000 -1.732756000000 -0.236213000000
 Cu 0.000000000000 2.156639000000 2.222906000000
 Cu 0.000000000000 0.000000000000 -1.428193000000

38

12.608357499 mol_0014.out

Cu 0.490434000000 0.660951000000 1.214726000000
 Cu 0.041111000000 -2.415770000000 -4.048698000000
 Cu 2.747884000000 -0.456741000000 1.297885000000
 Cu -0.957160000000 4.432673000000 0.000000000000
 Cu 2.933411000000 -2.548900000000 0.000000000000
 Cu -1.194825000000 -0.252714000000 4.080055000000
 Cu 0.041111000000 -2.415770000000 4.048698000000
 Cu 0.805645000000 -1.392475000000 0.000000000000
 Cu -3.117346000000 -1.304844000000 1.303217000000
 Cu -1.764792000000 3.196993000000 -2.011399000000
 Cu -3.407687000000 0.940158000000 0.000000000000
 Cu -0.655918000000 -3.746245000000 -2.060681000000
 Cu 2.339459000000 1.705216000000 -2.439606000000
 Cu 2.575996000000 3.985858000000 0.000000000000
 Cu -0.655918000000 -3.746245000000 2.060681000000
 Cu -3.117346000000 -1.304844000000 -1.303217000000
 Cu -1.194825000000 -0.252714000000 -4.080055000000
 Cu 2.339459000000 1.705216000000 2.439606000000
 Cu -1.764792000000 3.196993000000 2.011399000000
 Cu -2.043536000000 0.789376000000 2.053256000000
 Cu -1.485285000000 -2.694813000000 0.000000000000
 Cu -2.043536000000 0.789376000000 -2.053256000000
 Cu 1.222736000000 -0.357953000000 3.292161000000
 Cu -0.747423000000 -1.384082000000 2.044147000000
 Cu -0.084691000000 1.788565000000 -3.216016000000
 Cu -1.353109000000 -0.316455000000 0.000000000000
 Cu 0.697615000000 3.101250000000 -1.248349000000
 Cu 1.222736000000 -0.357953000000 -3.292161000000
 Cu -0.747423000000 -1.384082000000 -2.044147000000
 Cu 0.739459000000 -3.761653000000 0.000000000000
 Cu 0.490434000000 0.660951000000 -1.214726000000
 Cu 0.697615000000 3.101250000000 1.248349000000
 Cu 1.530052000000 -2.495519000000 2.066516000000
 Cu 2.747884000000 -0.456741000000 -1.297885000000
 Cu -1.219515000000 2.063010000000 0.000000000000
 Cu 2.446727000000 1.635631000000 0.000000000000
 Cu 1.530052000000 -2.495519000000 -2.066516000000
 Cu -0.084691000000 1.788565000000 3.216016000000

38

12.610240000 mol_0015.out

Cu	0.661737000000	1.214816000000	-0.489643000000
Cu	-2.416104000000	-4.048387000000	-0.041442000000
Cu	-0.456358000000	1.298349000000	-2.748137000000
Cu	4.432638000000	-0.000416000000	0.958471000000
Cu	-2.548506000000	0.000224000000	-2.933904000000
Cu	-0.252792000000	4.079621000000	1.195042000000
Cu	-2.415364000000	4.048809000000	-0.041520000000
Cu	-1.391187000000	0.000096000000	-0.806808000000
Cu	-1.305441000000	1.303821000000	3.116816000000
Cu	3.197018000000	-2.012629000000	1.763841000000
Cu	0.938092000000	-0.000081000000	3.408446000000
Cu	-3.746590000000	-2.060553000000	0.656123000000
Cu	1.705471000000	-2.439612000000	-2.339240000000
Cu	3.985098000000	0.000031000000	-2.576171000000
Cu	-3.746221000000	2.061255000000	0.656151000000
Cu	-1.305627000000	-1.303604000000	3.116823000000
Cu	-0.253465000000	-4.079581000000	1.195022000000
Cu	1.706049000000	2.439159000000	-2.339213000000
Cu	3.197322000000	2.011978000000	1.764034000000
Cu	0.789643000000	2.053007000000	2.043521000000
Cu	-2.694987000000	0.000241000000	1.485112000000
Cu	0.789325000000	-2.053163000000	2.043506000000
Cu	-0.357537000000	3.291929000000	-1.222920000000
Cu	-1.384112000000	2.043938000000	0.746749000000
Cu	1.788167000000	-3.216935000000	0.084344000000
Cu	-0.316686000000	0.000016000000	1.353009000000
Cu	3.101455000000	-1.248427000000	-0.697085000000
Cu	-0.358194000000	-3.291889000000	-1.222891000000
Cu	-1.384471000000	-2.043712000000	0.746778000000
Cu	-3.760542000000	0.000364000000	-0.739288000000
Cu	0.661538000000	-1.214962000000	-0.489649000000
Cu	3.101656000000	1.247976000000	-0.696854000000
Cu	-2.495493000000	2.066527000000	-1.530228000000
Cu	-0.456629000000	-1.298300000000	-2.748144000000
Cu	2.063161000000	-0.000218000000	1.221068000000
Cu	1.635141000000	-0.000201000000	-2.445930000000
Cu	-2.495903000000	-2.066099000000	-1.530218000000
Cu	1.788697000000	3.216615000000	0.084429000000

38

14.035292499 mol_0016.out

Cu	-1.052256000000	1.044878000000	3.371536000000
Cu	-1.616187000000	-0.195146000000	-1.252523000000
Cu	-1.816706000000	2.262978000000	1.271817000000
Cu	0.168498000000	-1.011714000000	-4.136016000000
Cu	0.190008000000	-1.181809000000	0.000000000000
Cu	-1.052256000000	1.044878000000	-3.371536000000
Cu	2.883659000000	1.294164000000	-2.050286000000
Cu	4.073968000000	-0.704254000000	-1.243667000000
Cu	-1.616187000000	-0.195146000000	1.252523000000
Cu	0.767182000000	-0.057525000000	2.037591000000
Cu	-0.135534000000	3.590639000000	0.000000000000
Cu	-2.204238000000	-1.146248000000	3.351462000000
Cu	0.168498000000	-1.011714000000	4.136016000000
Cu	2.644228000000	-0.831851000000	3.314148000000
Cu	2.031818000000	-2.125272000000	1.274870000000
Cu	-3.398127000000	0.846340000000	2.499066000000

Cu	-1.910493000000	-2.392712000000	0.000000000000
Cu	-3.398127000000	0.846340000000	-2.499066000000
Cu	0.601856000000	2.415250000000	2.056156000000
Cu	-3.522549000000	0.909687000000	0.000000000000
Cu	0.364766000000	-3.506967000000	0.000000000000
Cu	-0.384193000000	-2.311678000000	2.073765000000
Cu	-3.753807000000	-1.254323000000	-1.247595000000
Cu	-1.816706000000	2.262978000000	-1.271817000000
Cu	4.073968000000	-0.704254000000	1.243667000000
Cu	2.258432000000	0.103875000000	0.000000000000
Cu	1.357355000000	1.162590000000	4.031350000000
Cu	0.017510000000	1.196017000000	0.000000000000
Cu	1.357355000000	1.162590000000	-4.031350000000
Cu	-0.384193000000	-2.311678000000	-2.073765000000
Cu	2.644228000000	-0.831851000000	-3.314148000000
Cu	0.767182000000	-0.057525000000	-2.037591000000
Cu	-3.753807000000	-1.254323000000	1.247595000000
Cu	2.031818000000	-2.125272000000	-1.274870000000
Cu	0.601856000000	2.415250000000	-2.056156000000
Cu	2.883659000000	1.294164000000	2.050286000000
Cu	-2.204238000000	-1.146248000000	-3.351462000000
Cu	2.131754000000	2.504889000000	0.000000000000

Appendix F: XYZ atomic coordiantes at B3PW91/def2-SVP level of theory

38

0.000000000 B3PW91/def2-SVP_0000.out
Cu -2.963703000000 -2.066066000000 -1.176713000000
Cu 1.757807000000 -1.330766000000 0.021325000000
Cu -0.711140000000 -2.052754000000 -2.441671000000
Cu 4.039978000000 1.183631000000 0.944558000000
Cu 0.000004000000 0.000034000000 1.145773000000
Cu 3.612560000000 -0.070443000000 -1.176119000000
Cu 1.183124000000 3.412971000000 -1.176385000000
Cu 0.122815000000 4.207722000000 0.944169000000
Cu -0.722457000000 -2.083182000000 0.021582000000
Cu -2.204776000000 0.043067000000 0.022032000000
Cu -2.172348000000 0.042371000000 -2.441606000000
Cu -2.572864000000 -3.331911000000 0.944292000000
Cu -1.829251000000 -1.276275000000 2.190085000000
Cu -3.963903000000 1.417308000000 0.944229000000
Cu -2.440488000000 3.429228000000 0.944660000000
Cu -1.416260000000 -4.086208000000 -1.143821000000
Cu 0.648543000000 -2.133984000000 2.189984000000
Cu 3.448655000000 -2.609514000000 -1.143636000000
Cu -4.323915000000 0.084367000000 -1.143625000000
Cu 1.049369000000 -3.457516000000 -1.176327000000
Cu -1.779112000000 1.345191000000 2.190164000000
Cu 0.000033000000 -0.000036000000 3.480514000000
Cu 2.374105000000 -3.476227000000 0.944588000000
Cu 1.732657000000 -1.310914000000 -2.441600000000
Cu -1.256013000000 4.138099000000 -1.143594000000
Cu -0.640408000000 2.109993000000 0.022042000000
Cu -4.015979000000 -1.261335000000 0.944683000000
Cu -0.000069000000 0.000420000000 -1.322404000000
Cu 3.547588000000 2.473400000000 -1.143439000000
Cu 2.229919000000 -0.042597000000 2.189882000000
Cu 2.507004000000 3.380520000000 0.944835000000
Cu 1.809145000000 1.260635000000 0.021665000000
Cu -0.041393000000 -4.208649000000 0.944935000000
Cu 0.729651000000 2.107616000000 2.189866000000
Cu 1.782640000000 1.242423000000 -2.441696000000
Cu -2.880407000000 2.179969000000 -1.176639000000
Cu 3.989654000000 -1.339820000000 0.945070000000
Cu -0.630762000000 2.079232000000 -2.441656000000

38

0.953172499 B3PW91/def2-SVP_0001.out
Cu 3.435954000000 -1.116409000000 -1.176616000000
Cu 0.000000000000 2.204727000000 0.021459000000
Cu 2.066134000000 0.671328000000 -2.441553000000
Cu -3.381685000000 2.507302000000 0.944688000000
Cu 0.000000000000 0.000000000000 1.145877000000
Cu -2.123536000000 2.922797000000 -1.176616000000
Cu -3.435954000000 -1.116409000000 -1.176616000000
Cu -3.429584000000 -2.441374000000 0.944688000000
Cu 2.096820000000 0.681298000000 0.021459000000
Cu 1.295906000000 -1.783662000000 0.021459000000
Cu 1.276941000000 -1.757558000000 -2.441553000000
Cu 4.209596000000 -0.040746000000 0.944688000000
Cu 2.121315000000 -0.689257000000 2.190185000000
Cu 1.262085000000 -4.016154000000 0.944688000000

Cu	-1.262085000000	-4.016154000000	0.944688000000
Cu	4.113026000000	1.336403000000	-1.143689000000
Cu	1.311045000000	1.804499000000	2.190185000000
Cu	0.000000000000	4.324691000000	-1.143689000000
Cu	2.541990000000	-3.498749000000	-1.143689000000
Cu	2.123536000000	2.922797000000	-1.176616000000
Cu	0.000000000000	-2.230483000000	2.190185000000
Cu	0.000000000000	0.000000000000	3.480618000000
Cu	1.339588000000	3.990972000000	0.944688000000
Cu	0.000000000000	2.172462000000	-2.441553000000
Cu	-2.541990000000	-3.498749000000	-1.143689000000
Cu	-1.295906000000	-1.783662000000	0.021459000000
Cu	3.429584000000	-2.441374000000	0.944688000000
Cu	0.000000000000	0.000000000000	-1.322300000000
Cu	-4.113026000000	1.336403000000	-1.143689000000
Cu	-1.311045000000	1.804499000000	2.190185000000
Cu	-4.209596000000	-0.040746000000	0.944688000000
Cu	-2.096820000000	0.681298000000	0.021459000000
Cu	3.381685000000	2.507302000000	0.944688000000
Cu	-2.121315000000	-0.689257000000	2.190185000000
Cu	-2.066134000000	0.671328000000	-2.441553000000
Cu	0.000000000000	-3.612776000000	-1.176616000000
Cu	-1.339588000000	3.990972000000	0.944688000000
Cu	-1.276941000000	-1.757558000000	-2.441553000000

38

2.009882500	B3PW91/def2-SVP_0002.out		
Cu	2.235081000000	-0.677404000000	2.084444000000
Cu	-1.102557000000	0.054900000000	-4.238071000000
Cu	-1.102557000000	0.054900000000	4.238071000000
Cu	-0.244412000000	-2.205396000000	0.000000000000
Cu	-0.244494000000	1.784050000000	1.295935000000
Cu	0.961756000000	-1.334901000000	-4.108647000000
Cu	-1.102733000000	4.047768000000	1.257506000000
Cu	-1.102534000000	-4.014031000000	1.361705000000
Cu	-2.355422000000	-1.827638000000	1.327480000000
Cu	-2.355609000000	2.258764000000	0.000000000000
Cu	2.235081000000	-0.677404000000	-2.084444000000
Cu	-2.355582000000	0.697801000000	-2.148195000000
Cu	-2.355582000000	0.697801000000	2.148195000000
Cu	-2.355422000000	-1.827638000000	-1.327480000000
Cu	1.005985000000	1.119699000000	3.445411000000
Cu	1.005955000000	3.623303000000	0.000000000000
Cu	-0.244573000000	-0.681387000000	-2.097194000000
Cu	2.235103000000	1.773224000000	1.288238000000
Cu	2.235103000000	1.773224000000	-1.288238000000
Cu	0.961803000000	-4.320324000000	0.000000000000
Cu	-1.102733000000	4.047768000000	-1.257506000000
Cu	0.961741000000	3.495229000000	2.539184000000
Cu	0.961756000000	-1.334901000000	4.108647000000
Cu	3.472040000000	0.000089000000	0.000000000000
Cu	0.961741000000	3.495229000000	-2.539184000000
Cu	1.035302000000	0.000003000000	0.000000000000
Cu	-1.102534000000	-4.014031000000	-1.361705000000
Cu	1.005874000000	-2.931073000000	2.129625000000
Cu	1.005985000000	1.119699000000	-3.445411000000
Cu	-1.102689000000	2.446869000000	3.460671000000
Cu	-1.102689000000	2.446869000000	-3.460671000000
Cu	-1.102634000000	-2.535335000000	3.396393000000

Cu 1.005874000000 -2.931073000000 -2.129625000000
Cu -1.102634000000 -2.535335000000 -3.396393000000
Cu -0.244573000000 -0.681387000000 2.097194000000
Cu -0.244494000000 1.784050000000 -1.295935000000
Cu 2.235223000000 -2.191881000000 0.000000000000
Cu -1.494949000000 -0.000098000000 0.000000000000

38

2.400815000 B3PW91/def2-SVP_0003.out
Cu 1.766528000000 0.077673000000 3.446894000000
Cu 1.838190000000 0.080910000000 -0.000045000000
Cu 0.077740000000 -1.766492000000 3.446913000000
Cu -0.077751000000 1.766506000000 -3.446912000000
Cu 1.763047000000 1.925365000000 -1.779435000000
Cu 1.925345000000 -1.763064000000 -1.779452000000
Cu 0.080910000000 -1.838190000000 -0.000032000000
Cu -1.766562000000 -0.077671000000 -3.446876000000
Cu 1.763093000000 1.925351000000 1.779389000000
Cu -1.925323000000 1.763058000000 1.779439000000
Cu 0.000037000000 -0.000025000000 1.682692000000
Cu -0.077625000000 1.766462000000 3.446919000000
Cu -1.965931000000 3.488041000000 0.000044000000
Cu -3.488044000000 -1.965952000000 0.000067000000
Cu -1.838188000000 -0.080910000000 0.000026000000
Cu -0.156811000000 3.562953000000 1.737296000000
Cu -0.156860000000 3.562950000000 -1.737260000000
Cu 3.562973000000 0.156828000000 1.737221000000
Cu -3.562936000000 -0.156827000000 1.737311000000
Cu 1.925390000000 -1.763066000000 1.779369000000
Cu -3.647044000000 1.651996000000 0.000059000000
Cu -0.080909000000 1.838182000000 0.000010000000
Cu 3.488038000000 1.965934000000 -0.000040000000
Cu 3.647048000000 -1.652008000000 -0.000063000000
Cu -3.562987000000 -0.156844000000 -1.737200000000
Cu -1.763100000000 -1.925366000000 -1.779384000000
Cu -1.766426000000 -0.077689000000 3.446934000000
Cu 0.156876000000 -3.562943000000 1.737251000000
Cu 1.766417000000 0.077706000000 -3.446935000000
Cu -1.925395000000 1.763077000000 -1.779374000000
Cu 0.077620000000 -1.766441000000 -3.446908000000
Cu 0.156808000000 -3.562953000000 -1.737295000000
Cu 1.652006000000 3.647036000000 -0.000003000000
Cu -0.000036000000 0.000014000000 -1.682706000000
Cu 1.965955000000 -3.488038000000 -0.000047000000
Cu -1.651997000000 -3.647052000000 0.000026000000
Cu 3.562941000000 0.156852000000 -1.737322000000
Cu -1.763036000000 -1.925362000000 1.779427000000

38

2.730879998 B3PW91/def2-SVP_0004.out
Cu 1.882597000000 2.129958000000 1.676373000000
Cu -1.344741000000 3.519814000000 -0.719547000000
Cu 2.763553000000 2.763337000000 -0.756014000000
Cu 4.079672000000 0.704919000000 -1.669781000000
Cu -1.825838000000 0.692625000000 -0.133286000000
Cu 2.592148000000 -3.570855000000 -0.544308000000
Cu -0.514477000000 2.649208000000 1.801914000000
Cu -3.803023000000 -2.545118000000 -2.115802000000
Cu 2.542787000000 -2.963730000000 2.036260000000
Cu -3.269940000000 -1.516300000000 0.105120000000

Cu	0.105495000000	0.824799000000	3.446862000000
Cu	0.433737000000	-0.932992000000	-3.477843000000
Cu	1.713720000000	1.177590000000	-2.538706000000
Cu	-1.934983000000	-3.076574000000	1.906265000000
Cu	0.397790000000	-2.776614000000	-1.602484000000
Cu	2.462087000000	-1.297824000000	-1.938485000000
Cu	-3.832893000000	0.719471000000	1.127644000000
Cu	-1.687445000000	-1.404913000000	-2.115556000000
Cu	3.873859000000	-1.305304000000	0.289817000000
Cu	-3.621170000000	-0.035939000000	-1.832329000000
Cu	-1.947140000000	-3.530526000000	-0.700198000000
Cu	-2.315245000000	1.656362000000	3.147416000000
Cu	0.729291000000	3.543750000000	-2.205643000000
Cu	-1.950057000000	-0.554628000000	2.243282000000
Cu	-2.818606000000	2.919744000000	1.132268000000
Cu	4.189385000000	1.272501000000	0.880473000000
Cu	-1.163673000000	1.352090000000	-2.401880000000
Cu	0.885195000000	4.184092000000	0.351302000000
Cu	-3.371802000000	2.222983000000	-1.141821000000
Cu	2.401792000000	-0.331887000000	2.263422000000
Cu	0.278576000000	-3.765635000000	0.797566000000
Cu	0.264007000000	-1.789798000000	2.610879000000
Cu	-0.910641000000	-1.679981000000	0.346427000000
Cu	2.306248000000	0.474655000000	-0.162050000000
Cu	0.404958000000	2.005649000000	-0.469152000000
Cu	0.251085000000	-0.291179000000	-1.233171000000
Cu	0.243686000000	0.279173000000	1.210476000000
Cu	1.510005000000	-1.722922000000	0.384287000000

38

2.919129997	B3PW91/def2-SVP_0005.out		
Cu	-1.207309000000	-2.249324000000	-2.099540000000
Cu	-2.553408000000	-0.079343000000	2.099096000000
Cu	-1.987940000000	-3.704668000000	0.000010000000
Cu	-1.207294000000	-2.249303000000	2.099529000000
Cu	-0.135135000000	4.348504000000	1.260083000000
Cu	3.833218000000	-2.058011000000	1.259920000000
Cu	-2.553434000000	-0.079342000000	-2.099107000000
Cu	3.698293000000	2.291305000000	1.259681000000
Cu	0.135134000000	-4.348507000000	-1.260086000000
Cu	-0.135133000000	4.348510000000	-1.260087000000
Cu	-4.202513000000	-0.130263000000	0.000017000000
Cu	1.343863000000	-2.168928000000	2.099842000000
Cu	0.000000000000	0.000000000000	1.337808000000
Cu	1.987939000000	3.704667000000	0.000010000000
Cu	4.202510000000	0.130260000000	0.000018000000
Cu	2.213837000000	-3.574171000000	0.000007000000
Cu	-2.213836000000	3.574174000000	0.000007000000
Cu	2.553410000000	0.079340000000	2.099097000000
Cu	3.833248000000	-2.058021000000	-1.259889000000
Cu	1.207293000000	2.249304000000	2.099528000000
Cu	3.698331000000	2.291318000000	-1.259642000000
Cu	-1.343874000000	2.168947000000	-2.099850000000
Cu	-3.698296000000	-2.291308000000	1.259681000000
Cu	1.207308000000	2.249326000000	-2.099541000000
Cu	-3.833247000000	2.058021000000	-1.259882000000
Cu	0.135137000000	-4.348501000000	1.260083000000
Cu	-1.343860000000	2.168929000000	2.099840000000
Cu	-3.698333000000	-2.291321000000	-1.259643000000

Cu -3.833218000000 2.058011000000 1.259915000000
Cu 1.343877000000 -2.168947000000 -2.099852000000
Cu 2.553434000000 0.079340000000 -2.099108000000
Cu 0.000000000000 0.000000000000 -1.337839000000
Cu -0.072798000000 2.344484000000 -0.000011000000
Cu -1.993429000000 -1.234903000000 -0.000023000000
Cu -2.066580000000 1.109229000000 -0.000019000000
Cu 1.993425000000 1.234900000000 -0.000023000000
Cu 0.072796000000 -2.344481000000 -0.000011000000
Cu 2.066580000000 -1.109230000000 -0.000020000000

38

2.946739998 B3PW91/def2-SVP_0006.out

Cu 2.084683000000 0.677355000000 2.235209000000
Cu -4.238067000000 -0.055026000000 -1.102629000000
Cu 4.238067000000 -0.055026000000 -1.102629000000
Cu 0.000000000000 2.205357000000 -0.244668000000
Cu 1.296277000000 -1.784172000000 -0.244668000000
Cu -4.108780000000 1.335023000000 0.961854000000
Cu 1.257302000000 -4.047645000000 -1.102629000000
Cu 1.361968000000 4.013637000000 -1.102629000000
Cu 1.327722000000 1.827452000000 -2.355474000000
Cu 0.000000000000 -2.258855000000 -2.355474000000
Cu -2.084683000000 0.677355000000 2.235209000000
Cu -2.148299000000 -0.698025000000 -2.355474000000
Cu 2.148299000000 -0.698025000000 -2.355474000000
Cu -1.327722000000 1.827452000000 -2.355474000000
Cu 3.445437000000 -1.119490000000 1.005895000000
Cu 0.000000000000 -3.622747000000 1.005895000000
Cu -2.097420000000 0.681493000000 -0.244668000000
Cu 1.288405000000 -1.773338000000 2.235209000000
Cu -1.288405000000 -1.773338000000 2.235209000000
Cu 0.000000000000 4.320227000000 0.961854000000
Cu -1.257302000000 -4.047645000000 -1.102629000000
Cu 2.539365000000 -3.495137000000 0.961854000000
Cu 4.108780000000 1.335023000000 0.961854000000
Cu 0.000000000000 0.000000000000 3.471906000000
Cu -2.539365000000 -3.495137000000 0.961854000000
Cu 0.000000000000 0.000000000000 1.035123000000
Cu -1.361968000000 4.013637000000 -1.102629000000
Cu 2.129397000000 2.930864000000 1.005895000000
Cu -3.445437000000 -1.119490000000 1.005895000000
Cu 3.461012000000 -2.446556000000 -1.102629000000
Cu -3.461012000000 -2.446556000000 -1.102629000000
Cu 3.396325000000 2.535590000000 -1.102629000000
Cu -2.129397000000 2.930864000000 1.005895000000
Cu -3.396325000000 2.535590000000 -1.102629000000
Cu 2.097420000000 0.681493000000 -0.244668000000
Cu -1.296277000000 -1.784172000000 -0.244668000000
Cu 0.000000000000 2.191966000000 2.235209000000
Cu 0.000000000000 0.000000000000 -1.494815000000

38

3.288727499 B3PW91/def2-SVP_0007.out

Cu -1.768641000000 0.005711000000 3.447266000000
Cu -1.839297000000 0.005986000000 0.000000000000
Cu 0.005711000000 1.768641000000 3.447266000000
Cu -0.005711000000 -1.768641000000 -3.447266000000
Cu -1.852436000000 -1.840850000000 -1.778936000000
Cu -1.840850000000 1.852436000000 -1.778936000000

Cu	0.005986000000	1.839297000000	0.000000000000
Cu	1.768641000000	-0.005711000000	-3.447266000000
Cu	-1.852436000000	-1.840850000000	1.778936000000
Cu	1.840850000000	-1.852436000000	1.778936000000
Cu	0.000000000000	0.000000000000	1.683808000000
Cu	-0.005711000000	-1.768641000000	3.447266000000
Cu	1.800221000000	-3.577993000000	0.000000000000
Cu	3.577993000000	1.800221000000	0.000000000000
Cu	1.839297000000	-0.005986000000	0.000000000000
Cu	-0.011405000000	-3.563935000000	1.736603000000
Cu	-0.011405000000	-3.563935000000	-1.736603000000
Cu	-3.563935000000	0.011405000000	1.736603000000
Cu	3.563935000000	-0.011405000000	1.736603000000
Cu	-1.840850000000	1.852436000000	1.778936000000
Cu	3.567682000000	-1.820760000000	0.000000000000
Cu	-0.005986000000	-1.839297000000	0.000000000000
Cu	-3.577993000000	-1.800221000000	0.000000000000
Cu	-3.567682000000	1.820760000000	0.000000000000
Cu	3.563935000000	-0.011405000000	-1.736603000000
Cu	1.852436000000	1.840850000000	-1.778936000000
Cu	1.768641000000	-0.005711000000	3.447266000000
Cu	0.011405000000	3.563935000000	1.736603000000
Cu	-1.768641000000	0.005711000000	-3.447266000000
Cu	1.840850000000	-1.852436000000	-1.778936000000
Cu	0.005711000000	1.768641000000	-3.447266000000
Cu	0.011405000000	3.563935000000	-1.736603000000
Cu	-1.820760000000	-3.567682000000	0.000000000000
Cu	0.000000000000	0.000000000000	-1.683808000000
Cu	-1.800221000000	3.577993000000	0.000000000000
Cu	1.820760000000	3.567682000000	0.000000000000
Cu	-3.563935000000	0.011405000000	-1.736603000000
Cu	1.852436000000	1.840850000000	1.778936000000

38

3.328887499	B3PW91/def2-SVP_0008.out		
Cu	2.240200000000	1.224155000000	2.099540000000
Cu	0.060179000000	2.553931000000	-2.099096000000
Cu	3.689645000000	2.015686000000	0.000000000000
Cu	2.240200000000	1.224155000000	-2.099540000000
Cu	-4.349396000000	0.102498000000	-1.260083000000
Cu	2.086720000000	-3.817666000000	-1.259920000000
Cu	0.060179000000	2.553931000000	2.099096000000
Cu	-2.263487000000	-3.715384000000	-1.259681000000
Cu	4.349396000000	-0.102498000000	1.260083000000
Cu	-4.349396000000	0.102498000000	1.260083000000
Cu	0.098721000000	4.203372000000	0.000000000000
Cu	2.178952000000	-1.327548000000	-2.099842000000
Cu	0.000000000000	0.000000000000	-1.337808000000
Cu	-3.689645000000	-2.015686000000	0.000000000000
Cu	-0.098721000000	-4.203372000000	0.000000000000
Cu	3.590684000000	-2.186952000000	0.000000000000
Cu	-3.590684000000	2.186952000000	0.000000000000
Cu	-0.060179000000	-2.553931000000	-2.099096000000
Cu	2.086720000000	-3.817666000000	1.259920000000
Cu	-2.240200000000	-1.224155000000	-2.099540000000
Cu	-2.263487000000	-3.715384000000	1.259681000000
Cu	-2.178952000000	1.327548000000	2.099842000000
Cu	2.263487000000	3.715384000000	-1.259681000000
Cu	-2.240200000000	-1.224155000000	2.099540000000

Cu -2.086720000000 3.817666000000 1.259920000000
Cu 4.349396000000 -0.102498000000 -1.260083000000
Cu -2.178952000000 1.327548000000 -2.099842000000
Cu 2.263487000000 3.715384000000 1.259681000000
Cu -2.086720000000 3.817666000000 -1.259920000000
Cu 2.178952000000 -1.327548000000 2.099842000000
Cu -0.060179000000 -2.553931000000 2.099096000000
Cu 0.000000000000 0.000000000000 1.337808000000
Cu -2.344964000000 0.055202000000 0.000000000000
Cu 1.219908000000 2.002640000000 0.000000000000
Cu -1.124707000000 2.058197000000 0.000000000000
Cu -1.219908000000 -2.002640000000 0.000000000000
Cu 2.344964000000 -0.055202000000 0.000000000000
Cu 1.124707000000 -2.058197000000 0.000000000000
38
3.719819999 B3PW91/def2-SVP_0009.out
Cu -3.571762000000 1.809671000000 0.000000000000
Cu 0.000000000000 1.835970000000 0.000000000000
Cu -3.563116000000 0.000000000000 1.737394000000
Cu 3.563116000000 0.000000000000 -1.737394000000
Cu 1.845427000000 1.845427000000 -1.779671000000
Cu 1.845427000000 1.845427000000 1.779671000000
Cu 0.000000000000 0.000000000000 1.689627000000
Cu 3.571762000000 -1.809671000000 0.000000000000
Cu -1.845427000000 1.845427000000 -1.779671000000
Cu -1.845427000000 -1.845427000000 -1.779671000000
Cu -1.835970000000 0.000000000000 0.000000000000
Cu -3.563116000000 0.000000000000 -1.737394000000
Cu 0.000000000000 -1.769253000000 -3.449212000000
Cu 0.000000000000 -3.563116000000 1.737394000000
Cu 0.000000000000 -1.835970000000 0.000000000000
Cu -1.769253000000 0.000000000000 -3.449212000000
Cu 1.769253000000 0.000000000000 -3.449212000000
Cu -1.809671000000 3.571762000000 0.000000000000
Cu -1.809671000000 -3.571762000000 0.000000000000
Cu -1.845427000000 1.845427000000 1.779671000000
Cu 0.000000000000 -3.563116000000 -1.737394000000
Cu 0.000000000000 0.000000000000 -1.689627000000
Cu 0.000000000000 3.563116000000 -1.737394000000
Cu 0.000000000000 3.563116000000 1.737394000000
Cu 1.809671000000 -3.571762000000 0.000000000000
Cu 1.845427000000 -1.845427000000 1.779671000000
Cu -3.571762000000 -1.809671000000 0.000000000000
Cu -1.769253000000 0.000000000000 3.449212000000
Cu 3.571762000000 1.809671000000 0.000000000000
Cu 1.845427000000 -1.845427000000 -1.779671000000
Cu 3.563116000000 0.000000000000 1.737394000000
Cu 1.769253000000 0.000000000000 3.449212000000
Cu 0.000000000000 1.769253000000 -3.449212000000
Cu 1.835970000000 0.000000000000 0.000000000000
Cu 0.000000000000 1.769253000000 3.449212000000
Cu 0.000000000000 -1.769253000000 3.449212000000
Cu 1.809671000000 3.571762000000 0.000000000000
Cu -1.845427000000 -1.845427000000 1.779671000000
38
3.978977500 B3PW91/def2-SVP_0010.out
Cu 0.000000000000 -2.552852000000 2.099540000000
Cu 2.212383000000 -1.277320000000 -2.099096000000

Cu 0.000000000000 -4.204339000000 0.000000000000
Cu 0.000000000000 -2.552852000000 -2.099540000000
Cu 2.175372000000 3.767692000000 -1.260083000000
Cu -4.350603000000 0.000082000000 -1.260083000000
Cu 2.212383000000 -1.277320000000 2.099096000000
Cu -2.175372000000 3.767692000000 -1.260083000000
Cu -2.175231000000 -3.767774000000 1.260083000000
Cu 2.175372000000 3.767692000000 1.260083000000
Cu 3.641231000000 -2.102266000000 0.000000000000
Cu -2.212383000000 -1.277320000000 -2.099096000000
Cu 0.000000000000 0.000000000000 -1.337808000000
Cu 0.000000000000 4.204531000000 0.000000000000
Cu -3.641065000000 2.102170000000 0.000000000000
Cu -3.641231000000 -2.102266000000 0.000000000000
Cu 3.641065000000 2.102170000000 0.000000000000
Cu -2.210835000000 1.276426000000 -2.099540000000
Cu -4.350603000000 0.000082000000 1.260083000000
Cu 0.000000000000 2.554640000000 -2.099096000000
Cu -2.175372000000 3.767692000000 1.260083000000
Cu 2.210835000000 1.276426000000 2.099540000000
Cu 2.175231000000 -3.767774000000 -1.260083000000
Cu 0.000000000000 2.554640000000 2.099096000000
Cu 4.350603000000 0.000082000000 1.260083000000
Cu -2.175231000000 -3.767774000000 -1.260083000000
Cu 2.210835000000 1.276426000000 -2.099540000000
Cu 2.175231000000 -3.767774000000 1.260083000000
Cu 4.350603000000 0.000082000000 -1.260083000000
Cu -2.212383000000 -1.277320000000 2.099096000000
Cu -2.210835000000 1.276426000000 2.099540000000
Cu 0.000000000000 0.000000000000 1.337808000000
Cu 1.172793000000 2.031369000000 0.000000000000
Cu 1.172821000000 -2.031354000000 0.000000000000
Cu 2.345614000000 -0.000016000000 0.000000000000
Cu -1.172793000000 2.031369000000 0.000000000000
Cu -1.172821000000 -2.031354000000 0.000000000000
Cu -2.345614000000 -0.000016000000 0.000000000000

38

4.384342500 B3PW91/def2-SVP_0011.out
Cu 1.276478000000 -2.210925000000 2.099554000000
Cu 2.552956000000 0.000000000000 -2.099554000000
Cu 2.102153000000 -3.641035000000 0.000000000000
Cu 1.276478000000 -2.210925000000 -2.099554000000
Cu 0.000000000000 4.350864000000 -1.259862000000
Cu -3.767959000000 -2.175432000000 -1.259862000000
Cu 2.552956000000 0.000000000000 2.099554000000
Cu -3.767959000000 2.175432000000 -1.259862000000
Cu 0.000000000000 -4.350864000000 1.259862000000
Cu 0.000000000000 4.350864000000 1.259862000000
Cu 4.204305000000 0.000000000000 0.000000000000
Cu -1.276478000000 -2.210925000000 -2.099554000000
Cu 0.000000000000 0.000000000000 -1.337686000000
Cu -2.102153000000 3.641035000000 0.000000000000
Cu -4.204305000000 0.000000000000 0.000000000000
Cu -2.102153000000 -3.641035000000 0.000000000000
Cu 2.102153000000 3.641035000000 0.000000000000
Cu -2.552956000000 0.000000000000 -2.099554000000
Cu -3.767959000000 -2.175432000000 1.259862000000
Cu -1.276478000000 2.210925000000 -2.099554000000

Cu	-3.767959000000	2.175432000000	1.259862000000
Cu	1.276478000000	2.210925000000	2.099554000000
Cu	3.767959000000	-2.175432000000	-1.259862000000
Cu	-1.276478000000	2.210925000000	2.099554000000
Cu	3.767959000000	2.175432000000	1.259862000000
Cu	0.000000000000	-4.350864000000	-1.259862000000
Cu	1.276478000000	2.210925000000	-2.099554000000
Cu	3.767959000000	-2.175432000000	1.259862000000
Cu	3.767959000000	2.175432000000	-1.259862000000
Cu	-1.276478000000	-2.210925000000	2.099554000000
Cu	-2.552956000000	0.000000000000	2.099554000000
Cu	0.000000000000	0.000000000000	1.337686000000
Cu	0.000000000000	2.345454000000	0.000000000000
Cu	2.031223000000	-1.172727000000	0.000000000000
Cu	2.031223000000	1.172727000000	0.000000000000
Cu	-2.031223000000	1.172727000000	0.000000000000
Cu	0.000000000000	-2.345454000000	0.000000000000
Cu	-2.031223000000	-1.172727000000	0.000000000000

38

5.728447499	sapo_tripelte.out		
Cu	2.104971000000	1.810934000000	1.786347000000
Cu	-0.920785000000	3.673153000000	-0.570957000000
Cu	3.101279000000	2.494120000000	-0.597229000000
Cu	4.187925000000	0.350995000000	-1.608592000000
Cu	-1.740688000000	0.913318000000	-0.114805000000
Cu	2.214023000000	-3.720067000000	-0.761560000000
Cu	-0.254788000000	2.596591000000	1.879457000000
Cu	-4.147585000000	-1.963558000000	-2.099724000000
Cu	2.260582000000	-3.298281000000	1.829099000000
Cu	-3.456123000000	-1.316446000000	0.182859000000
Cu	0.136508000000	0.571013000000	3.473494000000
Cu	0.262347000000	-0.640973000000	-3.504849000000
Cu	1.883496000000	1.127917000000	-2.468600000000
Cu	-2.209859000000	-3.024099000000	1.757305000000
Cu	0.062092000000	-2.656015000000	-1.767559000000
Cu	2.307823000000	-1.396490000000	-2.021704000000
Cu	-3.782753000000	1.004111000000	1.091212000000
Cu	-1.920527000000	-0.982222000000	-2.101292000000
Cu	3.724253000000	-1.740556000000	0.215213000000
Cu	-3.856323000000	0.392576000000	-1.483624000000
Cu	-2.312115000000	-3.277106000000	-0.924262000000
Cu	-2.168717000000	1.674171000000	3.115662000000
Cu	1.152456000000	3.548818000000	-2.033777000000
Cu	-2.020892000000	-0.526310000000	2.207392000000
Cu	-2.535307000000	3.086668000000	1.171644000000
Cu	4.336054000000	0.718018000000	1.004649000000
Cu	-0.844051000000	1.681827000000	-2.342225000000
Cu	1.370527000000	4.041658000000	0.539962000000
Cu	-3.068092000000	2.628460000000	-1.178321000000
Cu	2.356616000000	-0.689556000000	2.250456000000
Cu	-0.073982000000	-3.819948000000	0.558015000000
Cu	0.087070000000	-1.975487000000	2.486229000000
Cu	-1.097536000000	-1.612902000000	0.243229000000
Cu	2.382211000000	0.245098000000	-0.129372000000
Cu	0.684806000000	1.982695000000	-0.354252000000
Cu	0.218590000000	-0.227528000000	-1.228178000000
Cu	0.263881000000	0.189080000000	1.214062000000
Cu	1.312613000000	-1.863675000000	0.284592000000

38

9.873712501 B3PW91/def2-SVP_0012.out

Cu	1.071797000000	1.039191000000	3.440671000000
Cu	1.670128000000	-0.195626000000	-1.292520000000
Cu	1.848556000000	2.272109000000	1.291536000000
Cu	-0.149249000000	-1.011549000000	-4.215538000000
Cu	-0.193359000000	-1.213779000000	0.000000000000
Cu	1.071797000000	1.039191000000	-3.440671000000
Cu	-2.926697000000	1.291384000000	-2.100001000000
Cu	-4.144992000000	-0.720394000000	-1.269998000000
Cu	1.670128000000	-0.195626000000	1.292520000000
Cu	-0.793115000000	-0.054366000000	2.103497000000
Cu	0.137050000000	3.640344000000	0.000000000000
Cu	2.237839000000	-1.153156000000	3.426281000000
Cu	-0.149249000000	-1.011549000000	4.215538000000
Cu	-2.707087000000	-0.827681000000	3.360700000000
Cu	-2.085961000000	-2.117034000000	1.295066000000
Cu	3.464683000000	0.842378000000	2.549647000000
Cu	1.953683000000	-2.401585000000	0.000000000000
Cu	3.464683000000	0.842378000000	-2.549647000000
Cu	-0.618647000000	2.422829000000	2.090675000000
Cu	3.583831000000	0.908208000000	0.000000000000
Cu	-0.373771000000	-3.539088000000	0.000000000000
Cu	0.393465000000	-2.314605000000	2.121537000000
Cu	3.823897000000	-1.259109000000	-1.260455000000
Cu	1.848556000000	2.272109000000	-1.291536000000
Cu	-4.144992000000	-0.720394000000	1.269998000000
Cu	-2.325514000000	0.108425000000	0.000000000000
Cu	-1.385560000000	1.158710000000	4.120699000000
Cu	-0.022367000000	1.227671000000	0.000000000000
Cu	-1.385560000000	1.158710000000	-4.120699000000
Cu	0.393465000000	-2.314605000000	-2.121537000000
Cu	-2.707087000000	-0.827681000000	-3.360700000000
Cu	-0.793115000000	-0.054366000000	-2.103497000000
Cu	3.823897000000	-1.259109000000	1.260455000000
Cu	-2.085961000000	-2.117034000000	-1.295066000000
Cu	-0.618647000000	2.422829000000	-2.090675000000
Cu	-2.926697000000	1.291384000000	2.100001000000
Cu	2.237839000000	-1.153156000000	-3.426281000000
Cu	-2.157666000000	2.523643000000	0.000000000000

38

10.693227499 B3PW91/def2-SVP_0013.out

Cu	0.675402000000	1.249212000000	-0.492475000000
Cu	-2.464758000000	-4.137839000000	-0.060290000000
Cu	-0.469092000000	1.310620000000	-2.773885000000
Cu	4.524120000000	-0.000617000000	0.955882000000
Cu	-2.607112000000	0.000336000000	-2.964050000000
Cu	-0.257136000000	4.145907000000	1.156285000000
Cu	-2.463644000000	4.138473000000	-0.060401000000
Cu	-1.429467000000	0.000153000000	-0.818879000000
Cu	-1.313961000000	1.317350000000	3.172039000000
Cu	3.254164000000	-2.031884000000	1.767070000000
Cu	0.960178000000	-0.000105000000	3.449731000000
Cu	-3.805944000000	-2.104611000000	0.640073000000
Cu	1.751484000000	-2.460017000000	-2.369341000000
Cu	4.026756000000	0.000043000000	-2.609294000000
Cu	-3.805391000000	2.105661000000	0.640093000000
Cu	-1.314228000000	-1.317023000000	3.172055000000

Cu	-0.258169000000	-4.145841000000	1.156297000000
Cu	1.752356000000	2.459324000000	-2.369303000000
Cu	3.254608000000	2.030918000000	1.767370000000
Cu	0.806373000000	2.105143000000	2.073751000000
Cu	-2.751648000000	0.000372000000	1.509650000000
Cu	0.805893000000	-2.105370000000	2.073744000000
Cu	-0.365018000000	3.340808000000	-1.235886000000
Cu	-1.432069000000	2.103715000000	0.772008000000
Cu	1.815697000000	-3.258006000000	0.089853000000
Cu	-0.330760000000	0.000030000000	1.404384000000
Cu	3.156046000000	-1.256726000000	-0.702840000000
Cu	-0.365992000000	-3.340762000000	-1.235855000000
Cu	-1.432615000000	-2.103358000000	0.772047000000
Cu	-3.810596000000	0.000538000000	-0.721979000000
Cu	0.675095000000	-1.249439000000	-0.492485000000
Cu	3.156350000000	1.256033000000	-0.702520000000
Cu	-2.531905000000	2.103095000000	-1.527759000000
Cu	-0.469486000000	-1.310553000000	-2.773893000000
Cu	2.119448000000	-0.000325000000	1.256405000000
Cu	1.661013000000	-0.000303000000	-2.479826000000
Cu	-2.532504000000	-2.102456000000	-1.527743000000
Cu	1.816512000000	3.257501000000	0.089966000000

38

10.695110000	B3PW91/def2-SVP_0014.out		
Cu	0.493648000000	0.674054000000	1.249181000000
Cu	0.059891000000	-2.464496000000	-4.138138000000
Cu	2.773432000000	-0.469529000000	1.309926000000
Cu	-0.953542000000	4.524129000000	0.000000000000
Cu	2.963496000000	-2.607632000000	0.000000000000
Cu	-1.155857000000	-0.257213000000	4.146794000000
Cu	0.059891000000	-2.464496000000	4.138138000000
Cu	0.817181000000	-1.431538000000	0.000000000000
Cu	-3.173134000000	-1.312900000000	1.316180000000
Cu	-1.768682000000	3.253869000000	-2.029986000000
Cu	-3.448350000000	0.963982000000	0.000000000000
Cu	-0.639505000000	-3.805505000000	-2.104754000000
Cu	2.369677000000	1.751035000000	-2.460192000000
Cu	2.608289000000	4.028800000000	0.000000000000
Cu	-0.639505000000	-3.805505000000	2.104754000000
Cu	-3.173134000000	-1.312900000000	-1.316180000000
Cu	-1.155857000000	-0.257213000000	-4.146794000000
Cu	2.369677000000	1.751035000000	2.460192000000
Cu	-1.768682000000	3.253869000000	2.029986000000
Cu	-2.073543000000	0.805649000000	2.105512000000
Cu	-1.509933000000	-2.751284000000	0.000000000000
Cu	-2.073543000000	0.805649000000	-2.105512000000
Cu	1.235758000000	-0.365563000000	3.341412000000
Cu	-0.773220000000	-1.432162000000	2.104178000000
Cu	-0.090414000000	1.816170000000	-3.256637000000
Cu	-1.404641000000	-0.330448000000	0.000000000000
Cu	0.703553000000	3.155639000000	-1.256914000000
Cu	1.235758000000	-0.365563000000	-3.341412000000
Cu	-0.773220000000	-1.432162000000	-2.104178000000
Cu	0.722224000000	-3.812153000000	0.000000000000
Cu	0.493648000000	0.674054000000	-1.249181000000
Cu	0.703553000000	3.155639000000	1.256914000000
Cu	1.527608000000	-2.531705000000	2.102999000000
Cu	2.773432000000	-0.469529000000	-1.309926000000

Cu	-1.253641000000	2.119179000000	0.000000000000
Cu	2.480492000000	1.662278000000	0.000000000000
Cu	1.527608000000	-2.531705000000	-2.102999000000
Cu	-0.090414000000	1.816170000000	3.256637000000